J. Fluid Mech. (1993), *vol.* 251, *pp.* 377–409

Time-dependent isolated anomalies in zonal flows

By KARL R. HELFRICH AND JOSEPH PEDLOSKY

Department of Physical Oceanography, Woods Hole Oceanographic Institution, Woods Hole, MA 02543, USA

(Received 9 September 1992 and in revised form 9 December 1992)

A theory is developed for time-dependent coherent structures in a marginally stable atmospheric zonal flow. The coherent structures have the form of solitary waves travelling in the zonal direction. Analytical solutions are found for stationary solitary waves but these are shown to be always unstable. The instability manifests itself either as a fission of the structure subsequently emitting two oppositely directed travelling solitary waves or as an implosion in which the structure becomes increasingly more narrow and intense. Which of the two occurs depends sensitively on initial conditions. These solitary waves are stable in head-on collisions *only* if their joint zonally integrated amplitude is less than a critical value; otherwise, the implosion instability occurs. General initial conditions can give rise to solitary waves which either split, implode, or break down to form a train of nonlinear wave packets. A scenario for the birth and decay of isolated disturbances is given, utilizing the slow parametric transit of the marginal stability curve of the background zonal flow.

1. Introduction

Coherent atmospheric flow patterns, i.e., those which last longer than the characteristic synoptic timescale of several days, have been the focus of much recent theoretical attention. The most well-known of these coherent patterns is the atmospheric blocking situation. This is the occurrence of a dipolar structure of high- and low-pressure centres arranged with the high poleward of the low so as to split the westerly flow in which it is embedded. Oceanic examples analogous to atmospheric blocking are less well documented, but given the dynamic similarities of the two systems on the synoptic scale, there is ample reason to believe the phenomenon should be common to both systems.

Theories for such coherent structures have been mainly developed along two lines. The first is the modon model (e.g. Haines & Marshall 1987 and references therein). The modon is a highly nonlinear, steady solution of the quasi-geostrophic equations on the β-plane in which nonlinearity balances the dispersive effect of β. In the analytical steady modon solution, the potential vorticity, q, is a linear function of the geostrophic stream function, ψ. The functional relationship differs though within and outside the dipolar zone of closed streamlines. That is, $q(\psi)$ is not a single-valued function.

A second class of solutions has been developed by Malanotte-Rizzoli and co-workers (see for example, Haines & Malanotte-Rizzoli 1991 and references therein) and is the focus of this paper. This model is characterized by *weakly* nonlinear solutions of the quasi-geostrophic potential vorticity equation. In the steady state, for which the solutions are found, $q(\psi)$ is a single-valued function. These solutions are of the form of long, stationary, solitary waves embedded in the westerly flow and the relevant governing equation is found to be of the Korteweg–de Vries (KdV) type:

$$A_{XX} - \kappa A + \tfrac{1}{2}\delta A^2 = 0, \tag{1.1}$$

which supports solutions localized in longitude X, of the form

$$A = \frac{3\kappa}{\delta}\operatorname{sech}^2\left(\frac{\kappa^{\frac{1}{2}}X}{2}\right). \tag{1.2}$$

The parameters κ and δ are determined by the meridional structure of the undisturbed westerly current in which the stationary solitary wave is embedded. The meridional structure of the disturbance is determined by an associated eigenvalue problem (see below) and κ and δ depend fundamentally on certain details of the form of $q(\psi)$ and its derivatives. In particular, depending on

$$\Lambda = \partial q/\partial\psi, \tag{1.3}$$

and on $\partial\Lambda/\partial\psi$ for the undisturbed flow, the possible zonally isolated solutions can lead either to a blocking of the westerly flow ($\partial\Lambda/\partial\psi < 0$) or a local acceleration of the flow, the so-called jet streak ($\partial\Lambda/\partial\psi > 0$). There is some question whether the weakly nonlinear solutions are really adequate in the case of blocking since $q(\psi)$ may be indeterminable on closed streamlines, but Malanotte-Rizzoli has argued for the relevance of the solitary wave model in the initial stages of block formation.

Both theoretical developments, i.e. the KdV theory as well as the modon theory, are fundamentally stationary solutions of the potential vorticity equation, for which reason the structure function $q(\psi)$ arises naturally as an exact integral. Although some effort has been made to discuss the temporal development of the coherent structures, this has been done for either deeply stable flow or flows which are considerably supercritical for ordinary baroclinic instability (Malguzzi & Malanotte-Rizzoli 1985).

It occurred to us that it might be useful to re-examine the question of the *time-dependent* dynamics of these coherent structures in flows that are only *marginally* stable (or marginally unstable) in the belief that the atmospheric zonal flow is never really deeply stable (with regard to a standard instability criticality condition) and is held close to the marginal state by eddy fluxes of unstable waves. To this end we begin here with a re-examination of the KdV theory of Malanotte-Rizzoli in the context of the classical two-layer baroclinic model for those parameter values that render the zonal flow marginally critical. The precise sense of this marginality is developed below. We then consider localized coherent structures that can exist in these conditions and, in particular, we examine the evolutionary behaviour in time of the relevant solutions.

We find that when the background flow is slightly *subcritical* with regard to baroclinic instability the *stationary KdV solutions are always unstable.* We actually consider this a point *in favour* of the original theory for it yields a finite lifetime for the stationary solutions and demonstrates the slow dissolution of the coherent structure. Our theory also allows the background flow to evolve from an unstable to a stable state and this, in turn, allows the flow a natural method to grow certain 'seed' disturbances into full-fledged coherent structures which, if stationary, then eventually dissolve.

In §2 we develop the asymptotic theory which leads to a time-dependent partial differential equation, in time and longitude (x), for the amplitude of the coherent structure. The steady form of this equation recovers the form (1.1). Certain clarifications of the original development of the steady theory are naturally exposed in the time-dependent development. In particular, the necessity (see Malguzzi & Malanotte-Rizzoli 1985) of a *small* eigenvalue of the associated modal problem in y (latitude) is rendered more systematic. We develop the theory primarily for the case where the westerly flow is near-critical, but we also describe the governing equation when the flow is strongly stable. In the first case the governing PDE is second order in time while in the second, less interesting case, it is first order. In §3 we describe the

possible solutions of solitary wave type of the amplitude equation and where in parameter space they may be found. We find that the parameter space may be conveniently divided into four quadrants depending on the cross-stream scale and the super- or subcriticality of the flow. In only one of these quadrants can stable solitary wave solutions be found. The *stationary* KdV solutions in this quadrant represent the limiting solution of maximum amplitude. Slowly travelling solutions of smaller amplitude are also possible. In §4 we examine numerically the time-dependent behaviour of the analytical solutions. In particular, we find that the stationary KdV solution is always unstable. In some cases the instability manifests itself as a splitting of the original solitary wave followed by the slow propagation upstream and downstream of the resulting 'pieces'. In other cases, the instability manifests itself as the explosive growth of a narrow, stationary peak, rendering invalid our asymptotic theory. A numerical treatment of the linear stability of the solitary waves is presented in §5. We show that linear theory is an excellent predictor of the nonlinear development found in the preceding section. For each KdV solution, two instability modes are possible above a critical solitary wave amplitude. Each has the same growth rate and they differ only in the sign of their amplitude projection on the solitary wave. One sign leads to splitting, the other to explosive growth. Thus, within the asymptotic theory, the subsequent nonlinear evolution depends sensitively on the initial perturbation data.

In §6 we describe numerical experiments involving either the overtaking of one solitary wave by a faster wave or the head-on collision of two solitary waves. Confounding our initial intuition we find that the solitary waves are stable in the former case and unstable in the latter case. In §7 we describe a few experiments with more general initial conditions which demonstrate the range of behaviour already qualitatively encountered by the pure solitary wave. In §8 we describe a few calculations in which the *background* flow is allowed to evolve from an unstable to a stable setting, demonstrating the growth to finite amplitude of small disturbance 'seeds' and the subsequent production of solitary waves. In our final section, 9, we recapitulate our major results and describe the direction of future work.

Although certain aspects of the time-dependent theory are grossly simplified with respect to the natural atmosphere, it is clear that a rich array of time-dependent dynamical phenomena associated with the coherent structures exists in addition to that of the possible steady solutions. The steady solutions, while of considerable potential significance meteorologically, are seen to be special cases of a more general evolutionary behaviour. Indeed, for weak *subcriticality*, the completely steady solutions are not even stable and therefore not realizable. This underscores the incomplete picture that special nonlinear steady solutions may represent. The coherence associated with such structures may, in fact, be fleeting and the real question then is primarily the timescale associated with the decline and dissolution of the coherent structure.

2. The model

We start with the two-layer version of the quasi-geostrophic potential vorticity equation on the β-plane for flow within a zonal channel of width L. For simplicity we ignore dissipation, but it may easily be added if the dissipation of potential vorticity anomalies is proportional to the potential vorticity itself.

In non-dimensional units the quasi-geostrophic potential vorticity equation is

$$\frac{\partial}{\partial t}\tilde{q}_n + J(\psi_n, \tilde{q}_n) = 0, \quad n = 1, 2, \tag{2.1}$$

where $\tilde{q}_n$ is the potential vorticity, related to the geostrophic stream function ψ_n by

$$\tilde{q}_n = \psi_{nxx} + \psi_{nyy} + F(-1)^n(\psi_1 - \psi_2) + \beta y + \eta_B(y)\delta_{n2}. \tag{2.2}$$

The parameters F and β are

$$F = \frac{f_0^2 L^2}{g(\Delta\rho/\rho) D}, \quad \beta = \frac{\beta_* L^2}{U}, \tag{2.3a, b}$$

where f_0, g, $\Delta\rho/\rho$, D, and β_*, are, respectively, the Coriolis parameter, the acceleration due to gravity, the density difference between the layers divided by the mean density, the rest thickness of each layer, and the dimensional β-parameter. U is a characteristic scale of the background zonal flow which is used to scale the horizontal velocities and with L to yield a characteristic time, L/U, to scale t, while L scales x and y. The Jacobian $J(a, b)$ has its usual meaning, $a_x b_y - a_y b_x$. The index n refers to the layer; $n = 1$ is the upper layer, $n = 2$ is the lower layer.

In terms of ψ_n, the horizontal velocities are

$$u_n = -\psi_{ny}, \quad v_n = \psi_{nx}. \tag{2.4a, b}$$

The last term in (2.2) is a possible topographic contribution to the potential vorticity in the lower layer.

Solitary waves which are confined in x and which are nearly stationary with regard to the Earth frame for zonal flows independent of x require rather special background states. We define the background zonal flow in that state as $U_n^{(0)}(y)$ with an accompanying potential vorticity $Q_n^{(0)}(y)$. We allow, however, a small but significant variation about this special state. The non-dimensional parameter measuring the departure is Δ such that the total background state in the absence of any flow anomaly is

$$U_n = U_n^{(0)} + \Delta U_n^{(1)}, \quad \Delta \ll 1, \quad Q_n = Q_n^{(0)} + \Delta Q_n^{(1)}. \tag{2.5a, b}$$

The basic field, which is purely zonal, satisfies a variant of (2.1) in which the non-linear terms vanish automatically, and small forcing and dissipation terms previously neglected must be considered, i.e.,

$$\frac{\partial Q_n}{\partial t} = \mathscr{D}_n(Q_n) + F_n, \tag{2.6}$$

where $\mathscr{D}_n$ is a dissipation of potential vorticity and F_n is a potential vorticity forcing, possibly a function of time. We need not solve (2.6) since Q_n and U_n will be specified, but it is important to realize that conceptually (2.6) allows us to consistently choose $U_n^{(1)}$ and $Q_n^{(1)}$ to be slow functions of time, if desired, without affecting the fundamental mathematical development.

The anomalies we will solve for will be *nearly* stationary in a frame moving with a velocity c_0. This velocity will itself be determined as an eigenvalue of the fundamental eigenvalue problem described below. We place ourselves in the coordinate frame translating with velocity c_0 by rewriting (2.1) in terms of y, t and

$$X = x - c_0 t, \tag{2.7}$$

while the total stream function and potential vorticity are each the sum of the basic state and the anomaly, i.e.

$$\tilde{q}_n = Q_n(y) + \epsilon q_n, \quad \psi_n = -\int U_n \, dy + \epsilon\phi_n, \tag{2.8a, b}$$

where ϵ is a non-dimensional measure of the anomaly with respect to the background flow.

We suppose that the anomaly is slowly evolving in time and has a long scale in x. That is, the timescale is long compared with L/U and the x-scale is long compared with L. We make this manifest by looking for solutions for ϕ_n, which are functions of

$$\xi = \alpha X \quad \text{and} \quad T = \mu t, \tag{2.9a, b}$$

where α and μ are both small with respect to unity. Writing

$$q_n = p_n + \alpha^2 \phi_{n\xi\xi}, \quad p_n \equiv \phi_{nyy} + F(-1)^n(\phi_1 - \phi_2), \tag{2.10a, b}$$

we rewrite (2.1) as

$$\begin{aligned}\mu(\partial/\partial T)(p_n + \alpha^2\phi_{n\xi\xi}) + (U_n^{(0)} - c_0)\alpha(p_n + \alpha^2\phi_{n\xi\xi})_\xi \\ + \alpha\phi_{n\xi}(\partial Q_n^{(0)}/\partial y + \Delta(\partial Q_n^{(1)}/\partial y)) + \alpha\Delta U_n^{(1)}(p_n + \alpha^2\phi_{n\xi\xi})_\xi \\ + \epsilon\alpha J(\phi_n, p_n + \alpha^2\phi_{n\xi\xi}) = 0,\end{aligned} \tag{2.11}$$

where the Jacobian in (2.11) is with respect to the variables ξ and y. The parameters μ, α, ϵ, and Δ are all assumed small with respect to unity, and some relative ordering between them is necessary. However, the relevant ordering is more easily understood as the analysis develops. For the moment, we need only assume that

$$\mu \ll \alpha, \tag{2.12}$$

which we may verify *a posteriori*. Then the lowest-order problem occurs at $0(\alpha)$. Writing each variable as, for example,

$$\phi_n = \phi_n^{(1)} + \nu\phi_n^{(2)} + \ldots, \tag{2.13}$$

where $\nu = \nu(\epsilon, \alpha, \Delta, \mu)$ is a small parameter, the problem for $\phi_n^{(1)}$ is

$$\frac{\partial}{\partial\xi}\left[(U_n^{(0)} - c_0)p_n^{(1)} + \frac{\partial Q_n^{(0)}}{\partial y}\phi_n^{(1)}\right] = 0. \tag{2.14}$$

For disturbances which are localized, $p_n^{(1)}$ and $\phi_n^{(1)}$ vanish at $\xi = \pm\infty$ so that (2.14) becomes

$$p_n^{(1)} - \kappa_n\phi_n^{(1)} = 0, \tag{2.15}$$

where $p_n^{(1)} = \phi_{nyy}^{(1)} + F(-1)^n(\phi_1^{(1)} - \phi_2^{(1)})$ and

$$\kappa_n \equiv -Q_{ny}^{(0)}/(U_n^{(0)} - c_0). \tag{2.16}$$

In the case where $c_0 = 0$, κ_n is the baroclinic generalization of the function Λ described in the introduction. Note that (2.15) is an eigenvalue problem in y. The boundary conditions are

$$\phi_n^{(1)} = 0, \quad y = 0, 1. \tag{2.17}$$

In distinction to the eigenvalue problem described by Malguzzi & Malanotte-Rizzoli (1985), the x-wavenumber *does not appear* as the eigenvalue. Instead (2.15) consistently examines eigensolutions in the asymptotic limit of *zero* x-wavenumber and the question of whether the numerical eigenvalue discussed by Malguzzi & Malanotte-Rizzoli is small enough never arises. Instead, the proper eigenvalue for (2.15) is c_0, which is the phase speed of waves in the two-layer model in the limit of infinite zonal wavelength. For general $U_n(y)$, the eigenvalue problem must be solved numerically, but its general character can be inferred from the classical model of Phillips (1954). In general, for arbitrary F and β, there will be two values of c_0, $c_0^{(1)}$ and $c_0^{(2)}$, that will allow

(2.15) to be satisfied for each cross-stream mode. In common with the previous work of Malanotte-Rizzoli and co-workers, we focus on the *second* cross-stream mode for which the anomaly will consist of a meridionally dipolar pattern. As in the Phillips model, we imagine each eigenvalue c_0 to be a function of β for the second cross-stream mode, namely

$$c_0^{(1)} = c_0^{(1)}(\beta), \quad c_0^{(2)} = c_0^{(2)}(\beta).$$

We ask for that value of β for which the two values of c_0 coalesce such that

$$c_0^{(1)}(\beta) = c_0^{(2)}(\beta) \equiv c_0. \tag{2.18}$$

That value of β for which the coalescence occurs determines the criticality condition for the mode under consideration. We will suppose that (2.15) has been solved for that value of β which satisfies (2.18). If at the same time c_0 should vanish, the conditions required by the steady theory of Malguzzi & Malanotte-Rizzoli would be met. This last condition can always be arranged by adding a uniform barotropic flow to the system, which is Galilean invariant, in order to arrest the wave.

We can, in any case, always write the solution of (2.15) as

$$\phi_n^{(1)} = A(\xi, T)\, H_n(y), \tag{2.19}$$

where $H_n(y)$ is the eigensolution of (2.15) and $A(\xi, T)$ is its unknown amplitude, which needs to be determined by the subsequent development of the asymptotic solution.

In the case where the coalescence does not occur, and both $c_0^{(1)}$ and $c_0^{(2)}$ are real, a different asymptotic development occurs for which the mode is firmly stable. The equation in this less interesting and, we believe, less relevant case is developed in the Appendix.

Assuming then that (2.15), (2.17), and (2.18) are satisfied, we can move to the next order. We will be able to verify after the fact that

$$\mu \gg (\alpha\Delta, \alpha^3, \epsilon\alpha). \tag{2.20}$$

Hence at next order, i.e. $O(\nu)$,

$$(U_n^{(0)} - c_0)[p_n^{(2)} - \kappa_n \phi_n^{(2)}]_\xi = -\frac{\mu}{\alpha\nu}\frac{\partial}{\partial T} p_n^{(1)} = -\frac{\mu}{\alpha\nu}\kappa_n \frac{\partial \phi_n^{(1)}}{\partial T},$$

or

$$p_{n\xi}^{(2)} - \kappa_n \phi_{n\xi}^{(2)} = \frac{\mu}{\alpha\nu}\frac{1}{(U_n^{(0)} - c_0)^2}\frac{\partial Q_n^{(0)}}{\partial y}\frac{\partial \phi_n^{(1)}}{\partial T}. \tag{2.21}$$

Note that ν in (2.13) is $O(\mu/\alpha)$.

If (2.21) is multiplied by $\phi_n^{(1)}$, integration by parts and use of (2.15) yields the condition

$$0 = \frac{\mu}{\alpha\nu}\sum_{n-1}^{2}\int_0^1 \mathrm{d}y \frac{1}{2}\frac{\partial}{\partial T}(\phi_n^{(1)})^2 \frac{1}{(U_n^{(0)} - c_0)^2}\frac{\partial Q_n^{(0)}}{\partial y}. \tag{2.22}$$

In the absence of critical layers, i.e. if $U_n^{(0)} - c_0$ does not vanish for any y, so that our expansion (2.15) is uniformly valid in y, then the condition of coalescence of roots, (2.18), guarantees the satisfaction of (2.22), as the example of the Phillips model shows. Indeed, (2.22) is the asymptotic limit of the Rayleigh condition for instability as the stability curve is approached parametrically. The satisfaction of the solvability condition (2.22) guarantees the existence of a solution of (2.21) in the form

$$\frac{\partial \phi_n^{(2)}}{\partial \xi} = \frac{\mu}{\alpha\nu}\frac{\partial A}{\partial T} f_n^{(2)}(y), \quad n = 1, 2, \tag{2.23}$$

where the $f_n^{(2)}(y)$ satisfy the inhomogeneous equations

$$f_{nyy}^{(2)} + (-1)^n F(f_1^{(2)} - f_2^{(2)}) - \kappa_n f_n^{(2)} = -\frac{\kappa_n}{U_n^{(0)} - c_0} H_n, \tag{2.24}$$

$$f_n^{(2)} = 0, \quad y = 0, 1.$$

We suppose that (2.24) may be solved, for its particular structure will not concern us. Note again that $f_n^{(2)}$ will be non-singular as long as $U_n^{(0)} - c_0 \neq 0$.

At the next order, we obtain

$$\alpha\nu^2(U_n^{(0)} - c_0)\frac{\partial}{\partial\xi}[p_n^{(3)} - \kappa_n \phi_n^{(3)}] = -\mu\nu\frac{\partial}{\partial T}p_n^{(2)} - \alpha^3(U_n^{(0)} - c_0)\frac{\partial^3\phi_n^{(1)}}{\partial\xi^3}$$

$$-\alpha\Delta\frac{\partial}{\partial\xi}\left[\frac{\partial Q_n^{(1)}}{\partial y}\phi_n^{(1)} + U_n^{(1)} p_n^{(1)}\right] - \epsilon\alpha J(\phi_n^{(1)}, p_n^{(1)}), \tag{2.25}$$

which requires the following ordering between the parameters:

$$\mu = O(\alpha^2) = O(\epsilon) = O(\Delta). \tag{2.26}$$

It is natural to think of Δ, the measure of the departure of the basic flow from its long-wave instability threshold, as being the external parameter of the problem. The relation (2.26) shows how the natural timescale, zonal lengthscale and amplitude of the anomaly are each chosen such that there is a balance between linear dispersion, nonlinearity, and temporal evolution.

If (2.15), (2.19), (2.23), are used to evaluate the right-hand side of (2.25), and the same solvability condition is applied to (2.25) as was applied to (2.21), we obtain the governing amplitude equation for the anomaly, i.e.

$$\boxed{m_1 A_{TT} + m_2 A_{\xi\xi\xi\xi} + m_3 A_{\xi\xi} + \tfrac{1}{2}m_4(A^2)_{\xi\xi} = 0}, \tag{2.27}$$

where we have provisionally chosen the exact ordering $\mu = \alpha^2 = \epsilon = \Delta$. The coefficients m_j are given by

$$m_1 = \int_0^1 dy \sum_{n=1}^{2} \frac{H_n}{U_n^{(0)} - c_0}[f_{nyy}^{(2)} + (-1)^n F(f_1^{(2)} - f_2^{(2)})], \tag{2.28a}$$

$$m_2 = \int_0^1 dy \sum_{n=1}^{2} H_n^2, \tag{2.28b}$$

$$m_3 = \int_0^1 dy \sum_{n=1}^{2} H_n^2\left[\frac{1}{U_n^{(0)} - c_0}\frac{\partial Q_n^{(1)}}{\partial y} - \frac{U_n^{(1)}}{(U_n^{(0)} - c_0)^2}\frac{\partial Q_n^{(0)}}{\partial y}\right], \tag{2.28c}$$

$$m_4 = \int_0^1 dy \sum_{n=1}^{2} \frac{H_n^3}{U_n^{(0)} - c_0}\frac{d\kappa_n}{dy}. \tag{2.28d}$$

The m_j are generally just numbers whose magnitudes will not be of concern in this study. In fact, they could easily have been absorbed in the definitions of ϵ, α, and μ. However, their sign is of particular importance as will be demonstrated in the following section, so for the moment we prefer to represent the governing equation as (2.27). The coefficient m_3 is of particular interest. Reference to (2.5*a*, *b*) and (2.6) shows that m_3 may be specified as a function of time and consequently could change sign as the system crosses from sub- to supercriticality. The bracket in (2.28*c*), whose projection on the square of the eigenfunction yields m_3, may be interpreted to $O(\Delta)$ as

$$\Delta\kappa = -\left[\frac{\partial Q/\partial y}{U_n - c_0} - \frac{\partial Q^{(0)}/\partial y}{U_n^{(0)} - c_0}\right] = O(\Delta). \tag{2.29}$$

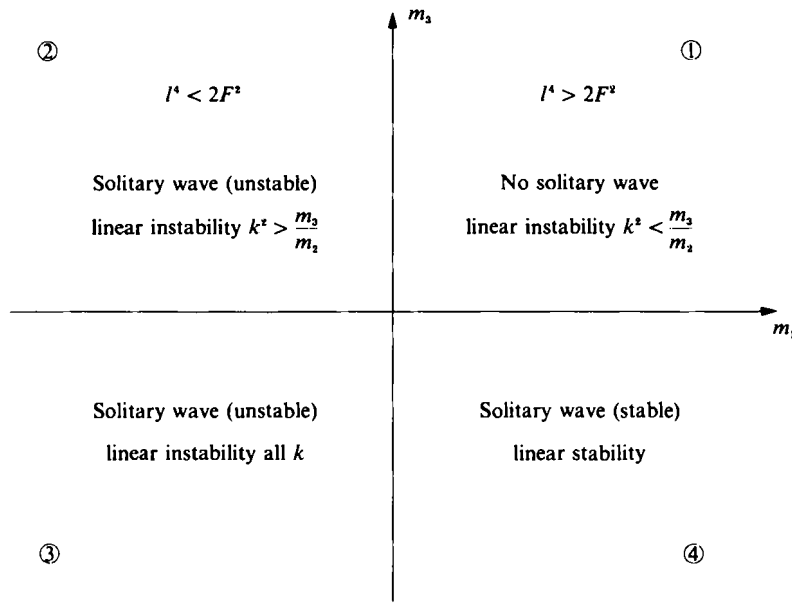

FIGURE 1. The four quadrants in the (m_1, m_3)-plane. For $m_1 > 0$ the meridional scale is expected to be short, for $m_1 < 0$ the meridional scale is large compared to a deformation radius. In quadrants 2, 3, and 4 solitary waves are possible. Only in quadrant 4 are such solutions not overwhelmed by linear instability of the background flow.

That is, m_3 is proportional to the small variation of κ obtained by altering the basic flow from that structure which yields the root coalescence (2.18) and, with the proper barotropic flow added, the stationarity of the anomaly. In the theory of Malguzzi & Malanotte-Rizzoli, it would be m_3 that plays the role of the small wavenumber appearing as the eigenvalue of their basic problem. However, we have preferred to consistently insist on a zero eigenvalue of the fundamental problem (2.15) and instead produce the equivalent linear term in the equation for the anomaly by controlling the departure of κ from its value at the coalescence point for c_0.

When the anomaly is entirely time-independent, (2.27) may be integrated twice in the zonal direction. For anomalies which vanish at $\pm\infty$ this yields

$$A_{\xi\xi} + \frac{m_3}{m_2} A + \frac{m_4}{m_2} \frac{A^2}{2} = 0, \tag{2.30}$$

which is exactly the equation obtained by Malguzzi & Malanotte-Rizzoli. Hence our time-dependent theory includes their steady solution as a special case.

It is, in general, hard to anticipate the signs of the m_j. The coefficient of the nonlinearity, m_4, depends critically on a delicate derivative of κ_n as described by Haines & Malanotte-Rizzoli. The sign of m_4 will determine whether the anomly yields a split jet or a jet intensification. Although of obvious meteorological importance, the sign of m_4 will play no role in the issues we shall discuss. The sign of m_1 can be estimated by evaluating the integral in (2.28a) in the case where U_1 and U_2 are constants. In that case, a little algebra shows

$$m_1 = +\frac{1}{4} \frac{\beta + F(U_1 - U_2)}{(U_1 - c_0)^3 (c_0 - U_2)} \left(\frac{l^4}{F^2}\right) (U_1 - U_2). \tag{2.31}$$

where l is the y-wavenumber of the cross-stream mode. For the dipolar solution $l = 2\pi$. The eigenvalue c_0 is given by

$$c_0 - U_2 = \frac{\beta F}{l^2(4F^2 - l^4)^{\frac{1}{2}}}\left[1 - \left(1 + \frac{l^2}{F}\right)\left(\frac{2F - l^2}{2F + l^2}\right)^{\frac{1}{2}}\right]. \tag{2.32}$$

For $l^2 > \sqrt{2F}$, $c_0 - U_2 > 0$ and m_1 is positive, while if $l^2 < \sqrt{2F}, m_1$ is negative. Naturally, the value of m_1 will, in general, depend on the structure of the basic flow, but we take this simple example as an indication that m_1 can be both positive and negative depending on the meridional scale of the anomaly with respect to the deformation radius. The sign of m_3, for the same example of uniform U_n, will be identical to that of m_1 if the variation of the basic state is such as to render it unstable with respect to small plane wave disturbances. Since m_2 is always positive, and m_4 affects only the sign of A, the time-dependent behaviour of the anomaly will depend on which of four sign combinations of m_1 and m_3 occur. In what follows, we will examine the behaviour of (2.27) and, in particular, determine in which quadrant, shown schematically in figure 1, stable, zonally limited anomalies are possible.

After deriving (2.27), we discovered that an equation of the same form had already been derived by Deininger (1980) for the case in which the U_n are exactly constant and $Q_n^{(1)}$ is produced by a small cross-stream topographic slope which is variable in y. From the above derivation, however, it is clear that the structural form of (2.27) is of far more general interest.

3. Solitary wave solutions

Solutions of (2.27) of the solitary wave type

$$A = A_0 \operatorname{sech}^2 \kappa(\xi - uT) \tag{3.1}$$

are possible as long as u, κ and A_0 satisfy

$$m_4 A_0 = -3m_3 - 3m_1 u^2, \tag{3.2a}$$

$$\kappa^2 = \frac{m_4}{m_2}\frac{A_0}{12}. \tag{3.2b}$$

Thus for a solitary wave solution to exist, $m_4 A_0$ must be positive (3.2b). It follows from (3.2a) that no solitary wave solution is possible in the quadrant $m_1 > 0, m_3 > 0$ of figure 1. If on the other hand, $m_1 < 0$ and $m_3 > 0$ (the second quadrant), only travelling solitary waves are possible for which

$$u^2 > m_3/|m_1|.$$

In the third quadrant, $m_3 < 0, m_1 < 0$ solitary waves are again possible, and the amplitude required *increases* with the speed of propagation of the anomaly. Finally, in the fourth quadrant $m_3 < 0, m_1 > 0$ and solitary waves are also possible, but the amplitude *decreases* with propagation speed. For stationary solitary waves (within the frame moving with c_0) m_3 must be negative. This is the requirement first discovered by Malguzzi & Malanotte-Rizzoli.

Although solitary solutions are possible in all quadrants except the first, we have found that violent instabilities destroy the solitary wave solution of quadrants 2 and 3.

To some extent this can be anticipated by a stability analysis of the linear part of (2.27). Ignoring the final, nonlinear term of (2.27), and searching for solutions of the type

$$A \sim e^{i(kx - \omega t)}, \tag{3.3}$$

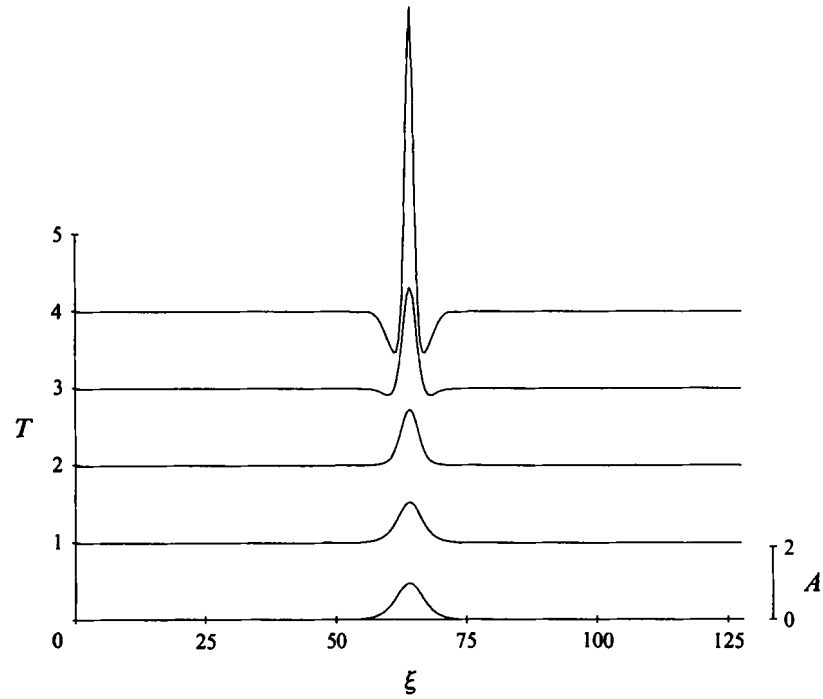

FIGURE 2. A numerical solution showing the explosive instability in quadrant 1, of an initial shape of the form of a solitary disturbance. The amplitude as a function of zonal position is shown at different times with the zero of amplitude offset so as to see the development with time of the spatial structure.

we obtain
$$\omega^2 = \left(\frac{m_2}{m_1}k^2 - \frac{m_3}{m_1}\right)k^2. \tag{3.4}$$

In the first three quadrants, as indicated in figure 1, there is always some range of wavenumber k which is linearly unstable. In all our numerical solutions, small noise present in the initial data rapidly swamped any other signal in all quadrants except quadrant 4 (see figure 2). Thus in the main, we shall focus our attention on the anomaly behaviour in quadrant 4. We emphasize that in this quadrant the background flow is slightly *subcritical* to small disturbances of the zonal flow.

We note that in the fourth quadrant the stationary solution found by Malanotte-Rizzoli and co-workers, be it of split jet or jet stream type, represents a limit point of the solitary wave form. With $u = 0$ the amplitude of the stationary solution reaches its maximum value, $m_4 A_0 = 3|m_3|$, and the solitary wave is at its most narrow, i.e. κ has also achieved its maximum with the stationary solution.

On the other hand, the maximum velocity of the solitary wave in the fourth quadrant occurs as A_0 goes to zero and is
$$(u)_{\max} = \pm(|m_3|/m_1)^{\frac{1}{2}}. \tag{3.5}$$
This should be compared with the group speed of small plane waves on the background flow which may be deduced from (3.4), i.e.
$$c_g \equiv \frac{\partial\omega}{\partial\kappa} = \pm\left(\frac{|m_3|}{m_1} + 2\frac{m_2}{m_1}k^2\right)\Big/\left(\frac{|m_3|}{m_1} + \frac{m_2}{m_1}k^2\right)^{\frac{1}{2}}, \tag{3.6}$$

which has $(u)_{\max}$ as its *minimum* value. Thus small, stable disturbances in this quadrant will always propagate faster than the solitary wave. This will allow irregular noise to pull away from the solitary anomaly leaving it isolated.

It is important to note the fact that our evolution equation is second-order in time. The solitary wave can propagate eastward or westward. In terms of our original variables x and t, this speed is $O(\mu/\alpha) = O(\alpha) = O(\Delta^{\frac{1}{2}})$. Thus truly stationary anomalies require first that c_0 vanish and then the velocity u represents a very slow movement of the anomaly with respect to this frame (in which c_0 vanishes). For a given solitary wave disturbance, the time taken for it to travel its own length, which we may take as the characteristic timescale for its disappearance, is $O(\Delta^{-1})$. Thus the closer the background state is to the critical curve, the longer the anomaly will remain in a given region. Of course, this estimate is based only on our scaling of x and t. In addition, the detailed question of the anomaly's persistence would depend on u. For example, if $u = 0$, the anomaly's duration is, in principle, infinite. However, as we shall now see, this stationary anomaly is unstable.

4. Behaviour of the solitary waves: numerical results

We have integrated (2.27) numerically using the explicit pseudo-spectral method of Fornberg & Whitman (1978) in which the spatial derivatives are evaluated using fast Fourier transforms. Time-stepping is done with a centred difference operator. The domain is periodic, but is made large enough so that the region of interest is essentially isolated. The numerical scheme was checked to ensure that mass (see below) was conserved (to 0.01% or better) in individual runs and that stable solitary waves propagated with a speed given by the theory (3.2*a*). The initial conditions for most runs were the analytical solitary wave with the addition of very small random perturbations.

Before describing our results, we first describe one global conservation principle we have succeeded in finding. A second conservation principle will be discussed below. If (2.27) is integrated over the finite-ξ interval, we obtain

$$\frac{\partial^2}{\partial T^2}\int_{-\infty}^{\infty} A\,\mathrm{d}\xi = 0, \tag{4.1}$$

assuming the disturbance vanishes at $\xi = \pm\infty$.

Hence the mass of the anomaly can, at most, grow linearly with time. However, it is not difficult to show, by returning to the original layer equations, that the linear growth is a spurious solution in the present asymptotic limit. This is connected with the requirement that the zonally averaged q_n in each layer be conserved for small-amplitude, zonally limited disturbances. In all our calculations $\partial A(0)/\partial T = 0$, initially, so then the mass will be conserved directly from (4.1).

In fact, we have taken the conservation of

$$m = \int_{-\infty}^{\infty} A\,\mathrm{d}\zeta = \text{constant}, \tag{4.2}$$

to be one of our chief diagnostics for the accuracy of our numerical integration. For the solitary wave solution, we find

$$m = \left(48\frac{m_2}{m_4}A_0\right)^{\frac{1}{2}}. \tag{4.3}$$

Figure 3 shows the numerical solution corresponding to an initial condition of a

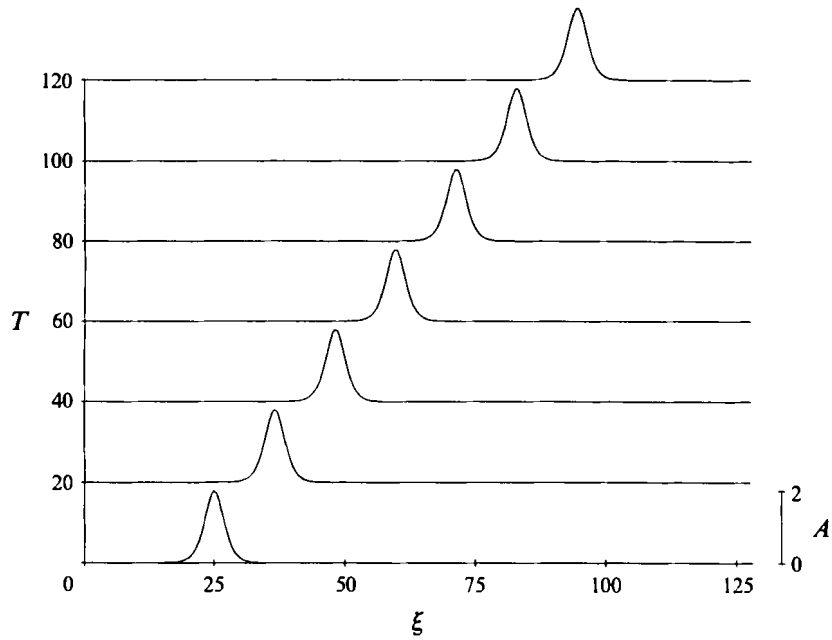

FIGURE 3. The stable propagation calculated numerically of the solitary wave with amplitude $A_0 = 2$.

solitary wave of amplitude $A_0 = 2$. For these calculations, all done in quadrant 4, $(m_1 > 0, m_3 < 0)$, we have chosen

$$\epsilon = -\Delta(m_3/m_4), \quad \alpha = (-\Delta(m_3/m_2))^{\frac{1}{2}}, \quad \mu = -\Delta m_3/m_1 m_2,$$

so that (2.27) can be put into the canonical form

$$A_{TT} - A_{\xi\xi} + A_{\xi\xi\xi\xi} + \tfrac{1}{2}(A^2)_{\xi\xi} = 0, \tag{4.4}$$

which is equivalent to setting

$$(m_1, m_2, m_3, m_4) = (1, 1, -1, 1),$$

in (2.27).

In this form (3.2) becomes

$$u^2 = 1 - \tfrac{1}{3}A_0, \quad \kappa^2 = \tfrac{1}{12}A_0. \tag{4.5a, b}$$

Hence $(A_0)_{\max} = 3$.

We see in figure 3 the propagation, without change of shape, of the solitary wave as predicted by the analytical solution.

On the other hand, if we start with the stationary solution for which $u = 0$ and $A_0 = 3$ and small random noise (the steady solution of the theory of Malguzzi & Malanotte-Rizzoli or Haines & Malanotte-Rizzoli for either the split jet or jet streak cases), we observe the unstable behaviour shown in figures 4(*a*) and 4(*b*). Either the solution splits apart yielding two solitary waves of lower amplitude, one travelling eastward and one travelling westward, as in figure 4(*a*), or equally likely, the instability manifests itself as the explosive growth of a stationary but narrowing peak, i.e. an implosion. In the latter case the narrowing is sufficient to compensate for the growth in amplitude so as to preserve the total mass (4.3). In the latter case, of course, eventually the resulting large amplitude and shortened zonal scale of the disturbance places the anomaly beyond the validity of the asymptotic theory. It is important to recall that this is an instability of the solitary wave. The background flow is definitely subcritical $(m_3 < 0)$.

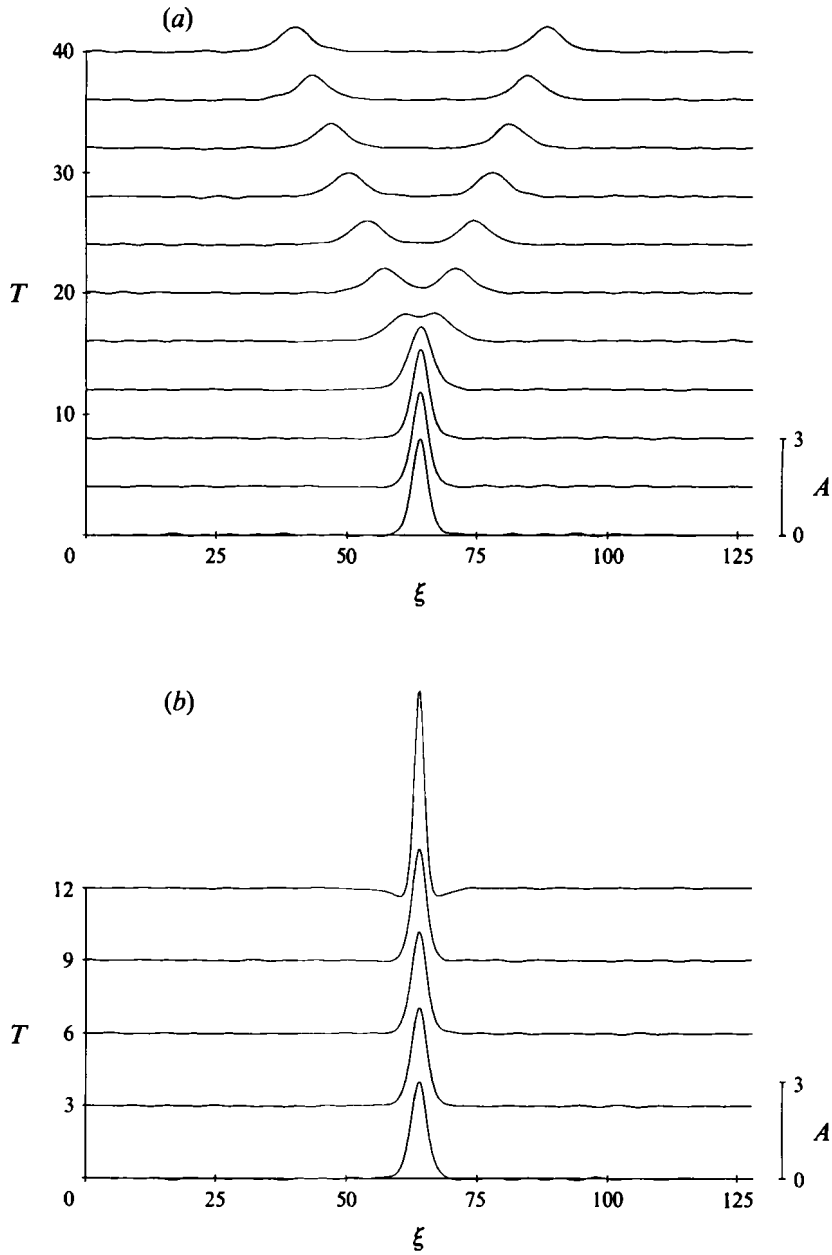

FIGURE 4. (*a*) The fission instability of the stationary solitary wave with $A_0 = 3$. (*b*) The explosive instability of the same solitary wave. Both runs had the same random perturbations superimposed on the solitary waves except that the sign of the perturbations was reversed between runs.

The instability is not limited to the stationary solution. Figure 5 shows the splitting instability for the slowly travelling solitary wave with $A_0 = 2.9$. No perturbations, other than numerical roundoff error, were introduced. In this case the solitary wave, which was originally travelling to the right, splits asymmetrically into two smaller-amplitude solitary disturbances. The larger, narrower disturbance moves in the original direction of propagation while a broader, lower-amplitude disturbance moves upstream. This instability is observed for $A_0 > 2.3$. Figure 6 shows a summary of our

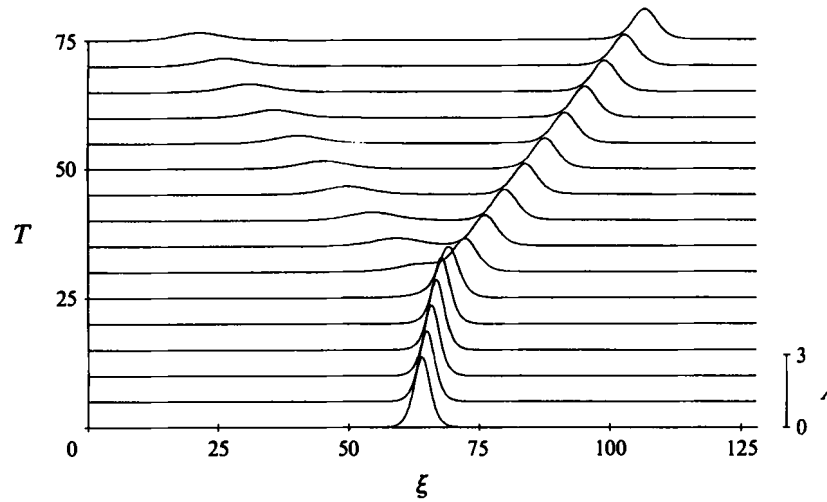

FIGURE 5. The fission instability of the rightward travelling solitary wave with $A_0 = 2.9$.

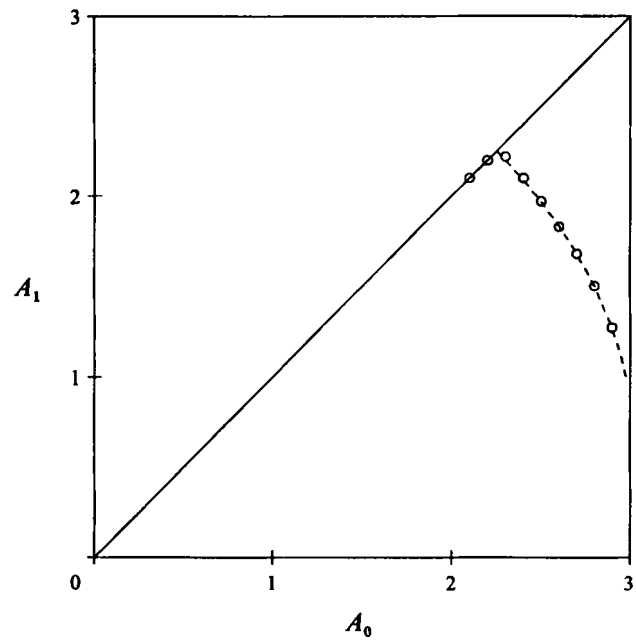

FIGURE 6. The solitary wave stability diagram in which the larger amplitude produced by fission is plotted against the initial amplitude. The circles show the numerical results and the dashed line is from the conservation laws (4.10) and (4.13).

calculations. On the abscissa, we place the amplitude of the initial solitary wave, and on the ordinate, the amplitude of the larger of the two waves formed by the splitting instability. At $A_0 \sim 2.3$, the larger amplitude of the emitted waves essentially matches the initial amplitude, and below this threshold the solitary wave is stable.

This initial amplitude and the amplitudes of the scattered solitary waves can be determined from a conservation law derived from (4.4). In a frame of reference moving at velocity u_0, we take

$$\zeta = \xi - u_0 T, \quad \tau = T,$$

and (4.4) then becomes

$$A_{\tau\tau} - 2u_0 A_{\zeta\tau} + (u_0^2 - 1) A_{\zeta\zeta} + A_{\zeta\zeta\zeta\zeta} + \tfrac{1}{2}(A^2)_{\zeta\zeta} = 0. \tag{4.6}$$

If (4.6) is multiplied by ζ, then integrated over the infinite ζ interval we obtain

$$\frac{\partial^2}{\partial\tau^2}\overline{\zeta A} + 2u_0 \frac{\partial}{\partial\tau}\bar{A} = 0 \tag{4.7}$$

assuming that the disturbance vanishes at $\zeta = \pm\infty$. The overbar signifies integration in ζ from $-\infty$ to $+\infty$.

As discussed earlier the mass ($\bar{A}$) is conserved for initial conditions in which $\partial\bar{A}(0)/\partial\tau = 0$. Thus (4.7) gives

$$\frac{\partial}{\partial\tau}\overline{\zeta A} = \text{constant}. \tag{4.8}$$

The moment $\overline{\zeta A}$ grows linearly with time. For the solitary wave solution to (4.4) given by (3.1) and (4.5*a*, *b*) of amplitude A_n and speed u_n, (4.8) can be evaluated to give

$$\begin{aligned}\frac{\partial}{\partial\tau}\overline{\zeta A} &= \frac{\partial}{\partial\tau}\int_{-\infty}^{\infty} \zeta A_n \operatorname{sech}^2 \kappa_n(\zeta - (u_n - u_0)\tau)\,\mathrm{d}\zeta \\ &= (u_n - u_0)\,4\sqrt{3}\,A_n^{\frac{1}{2}}.\end{aligned}$$

Integrating in τ gives

$$\overline{\zeta A} = (u_n - u_0)\,4\sqrt{3}\,A_n^{\frac{1}{2}}\tau. \tag{4.9}$$

Note that if $u_n = u_0$, $\overline{\zeta A} = 0$.

Guided by the numerical results (e.g. figure 5), we assume that the initial solitary wave of amplitude A_0 and speed u_0 splits into two solitary waves, A_1 which moves in the original direction of A_0 and A_2 which moves in the opposite direction. Conservation of mass gives

$$A_0^{\frac{1}{2}} = A_1^{\frac{1}{2}} + A_2^{\frac{1}{2}}. \tag{4.10}$$

Using the moment conservation law (4.9) with $u_0 = u_0$ gives

$$(u_1 - u_0)\,A_1^{\frac{1}{2}} + (u_2 - u_0)\,A_2^{\frac{1}{2}} = 0. \tag{4.11}$$

Mass conservation (4.10) can be used in (4.11) to obtain

$$u_0 A_0^{\frac{1}{2}} = u_1 A_1^{\frac{1}{2}} + u_2 A_2^{\frac{1}{2}}. \tag{4.12}$$

Equation (4.5*a*) is then used to eliminate u_n in favour of A_n and, recalling that $u_0, u_1 > 0$ and $u_2 < 0$, we find

$$(1 - \tfrac{1}{3}A_0)^{\frac{1}{2}} A_0^{\frac{1}{2}} = (1 - \tfrac{1}{3}A_1)^{\frac{1}{2}} A_1^{\frac{1}{2}} - (1 - \tfrac{1}{3}A_2)^{\frac{1}{2}} A_2^{\frac{1}{2}}. \tag{4.13}$$

Thus if A_0 is given, A_1 and A_2 can be determined from (4.10) and (4.13).

Near the critical point for splitting, $A_1 \to A_0$ and $A_2 \to 0$. Taking

$$A_1 = A_0 - \Delta; \quad \Delta \ll 1, \tag{4.14}$$

(4.10) gives

$$A_2 = \frac{\Delta^2}{4A_0} + O(\Delta^3). \tag{4.15}$$

This result shows right away the asymmetry of the two scattered waves. Now using (4.14) and (4.15) in (4.13) and dropping terms of $O(\Delta^2)$ or higher, we find that

$$\tfrac{4}{9}A_0^2 - A_0 = 0,$$

which gives the critical amplitude $A_{0c} = 2.25$. This agrees very well with the numerically determine value of $A_{0c} \approx 2.3$ shown in figure 6.

Also shown in figure 6 by the dashed line is the solution to the conservation

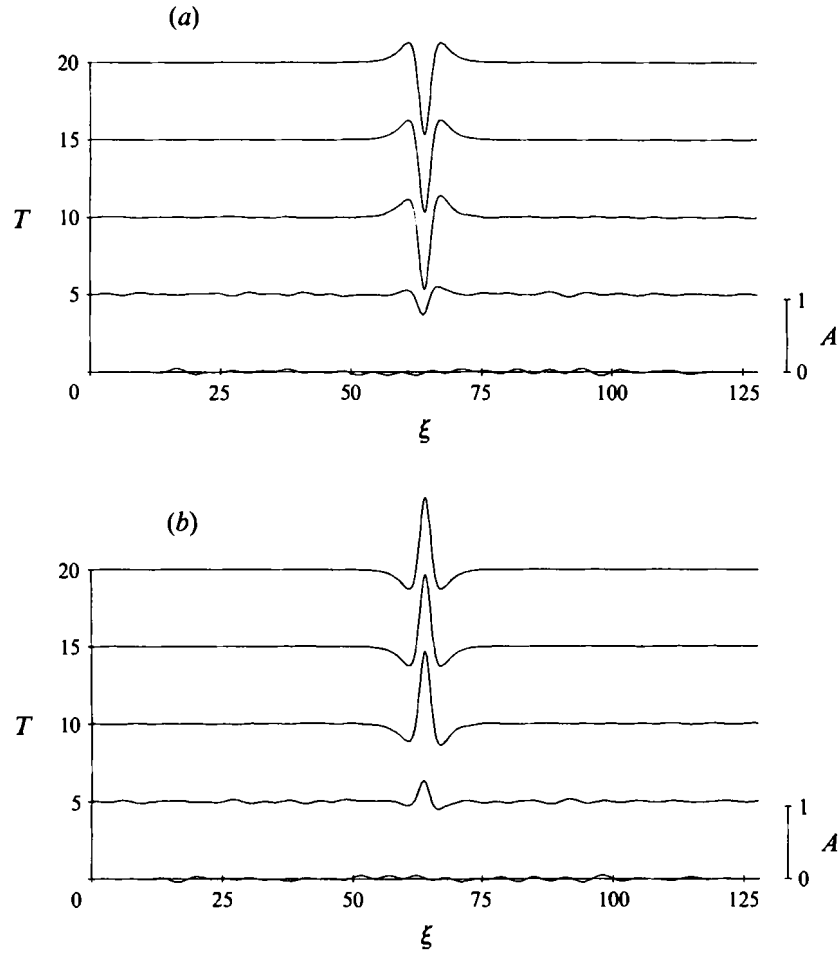

FIGURE 7(*a*,*b*). For caption see facing page.

conditions (4.10) and (4.13) for A_1 given the initial wave amplitude A_0. The agreement between the theory and the numerical results is excellent.

It follows that only slowly *propagating* solitary waves are stable. In particular, the stationary solution previously suggested as a candidate for long-lived coherent anomalies in atmospheric flows is, in fact, unstable and fleeting. As previously noted, however, the timescale for the splitting and subsequent departure of the pieces depends critically on the closeness of the flow to the critical curve of the background state. Hence, the breakdown of the steady solution can be very slow. We consider this an unexpected advantageous quality of the theory for it suggests a finite lifetime for the coherent anomalies independent of dissipative processes, depending instead on the ideal fluid dynamics which produce the anomaly.

5. Linear instability of the solitary wave solution

To understand and quantify the observed breakdown of the nonlinear solitary wave solutions, we have examined the linear stability of the solution (3.1) to small disturbances. Writing

$$A = A_S + a, \tag{5.1}$$

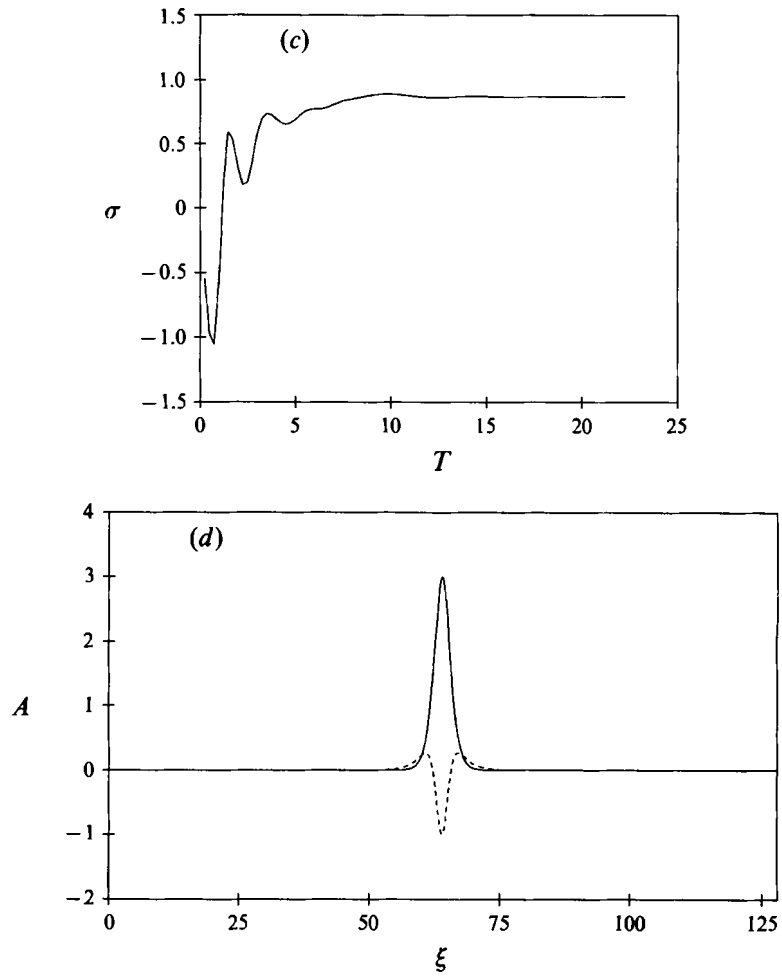

FIGURE 7. (*a*) The development of the linear instability fission mode for $A_0 = 3$. (*b*) The development of the explosion mode for $A_0 = 3$. (*c*) The time history of the growth rate. (*d*) The final normal mode shape (– – –) for the fission mode superimposed on the solitary wave (——). In (*a*) and (*b*) the plots have been normalized so that the solution has a maximum amplitude of 1, once the amplitude exceeds 1.

where A_S is the solitary wave solution and $a(\xi, T)$ is a superposed small-amplitude disturbance, we obtain the governing equation for $a(\xi, T)$ by putting (5.1) into (4.4). Keeping only linear terms, we obtain

$$a_{TT} - a_{\xi\xi} + a_{\xi\xi\xi\xi} + aA_{S\xi\xi} + a_{\xi\xi}A_S + 2a_\xi A_{S\xi} = 0. \tag{5.2}$$

We have integrated (5.2) subject to the initial condition

$$a(\xi, 0) = \sum_{i=1}^{N} a_0^{(i)} \cos(k_i \xi + \phi_i), \quad k_i = i\Delta k, \tag{5.3}$$

where $a_0^{(i)}$ and ϕ_i are the random amplitude and phase of the disturbance. Here $\Delta k = 2\pi/L_\xi$ and L_ξ is the size of the numerical domain. The number of waves N included in (5.3) was chosen such that $k_N \lesssim 1.2$. We chose $a_T(\xi, 0) = 0$. The solution

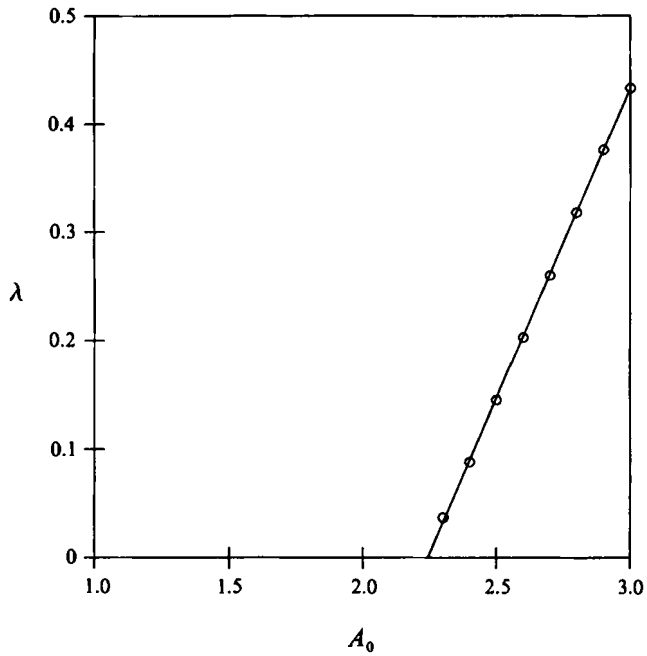

FIGURE 8. The linear stability diagram showing growth rate versus solitary wave amplitude. The circles are from the numerical calculations and the solid line is a linear fit to the results.

is calculated numerically using the same method as for the full nonlinear equation. The quantity

$$\sigma = \frac{\mathrm{d}}{\mathrm{d}T}\int_{-\infty}^{\infty} a^2 \mathrm{d}\xi \Big/ \int_{-\infty}^{\infty} a^2 \mathrm{d}\xi \tag{5.4}$$

is evaluated until σ becomes independent of time, i.e. $\sigma \to \sigma_\infty$. This yields the fastest growing mode of instability of the form

$$a = g(\xi - uT)\mathrm{e}^{\lambda T}, \tag{5.5}$$

where $\lambda = \frac{1}{2}\sigma_\infty$.

It follows from the invariance of (5.2) under the transformation $a \to -a$, that for every normal mode with growth rate λ, a second mode exists with the same λ for which $a \to -a$. Figure 7(*a*, *b*) shows the rise out of the initial random field of each of these disturbances, and figure 7(*c*) shows the stabilization of σ as a function of time for the run in figure 7(*a*). In figure 7(*d*), we superimpose the unstable normal mode on the initial solitary wave, here stationary for $A_0 = 3$. The linear mode as shown in figure 7(*d*) would tend to yield a depression, i.e. a nascent splitting in the original solitary wave. If instead the normal mode has the opposite sign, it would tend to enhance the magnitude of the peak value of the solitary wave. Indeed, if each calculation is carried into finite amplitude, the results shown in Figure 4(*a*, *b*) are obtained. That is, the occurrence of splitting or explosion of the unstable solitary wave depends on the sign of the instability mode which is excited. In particular, we have found empirically that the appropriate measure of the sign of the instability mode is determined by

$$S = \int_{-\infty}^{\infty} A_{\mathrm{S}}(\xi)\, a(\xi, 0)\, \mathrm{d}\xi, \tag{5.6}$$

that is, the initial projection of the perturbation on A_{S}. We have found that $S > 0$ (a

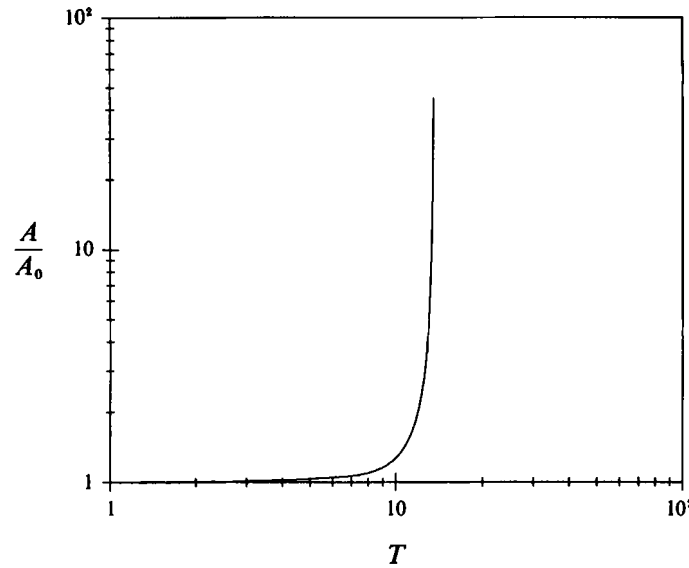

FIGURE 9. The temporal nonlinear behaviour of the maximum amplitude for a solitary wave with $A_0 = 3$.

linear positive mode) leads to a nonlinear explosive behaviour while $S < 0$ results in nonlinear splitting. Since S depends on details of the initial noise distribution, the finite-amplitude evolution of the solitary wave, when unstable, is extremely sensitive to initial data. Of course, in the case of $S > 0$, when explosive growth occurs, our asymptotic theory is unable to characterize the long-term behaviour of the unstable system.

As the amplitude of the perturbed solitary wave is reduced, the growth rate is also reduced. Figure 8 shows the result of our calculation of the growth rate. It appears that λ is a linear function of A_0 above a critical value $A_{0c} \sim 2.24$ such that

$$\lambda = 0.572(A_0 - A_{0c}). \tag{5.7}$$

This critical amplitude agrees very well with $A_{0c} = 2.25$ derived in the previous section from the conservation laws. The coincidence of the linear instability threshold and the finite-amplitude results summarized in figure 6 suggests that the linear instability develops spontaneously from the background noise, and the instability, rather than being equilibrated by nonlinear effects, is enhanced, leading to splitting or explosion. Figure 9 shows the behaviour in time of the peak amplitude for the case $A_0 = 3$. After a period of initial exponential growth, a nonlinear catastrophic growth occurs, well modelled by the equation

$$\frac{\mathrm{d}}{\mathrm{d}t}\left(\frac{A}{A_0}\right) = \lambda\frac{A}{A_0} + N\left(\frac{A}{A_0}\right)^3, \quad N > 0, \tag{5.8}$$

leading to the destruction of the initial solitary wave.

6. The collision of two solitary waves

As we have noted, completely stationary solitary waves are unstable and, depending on the initial data, may split and evolve into two travelling solitary waves. Hence if more than one initial anomaly is initially present on a latitude circle, it is likely that the

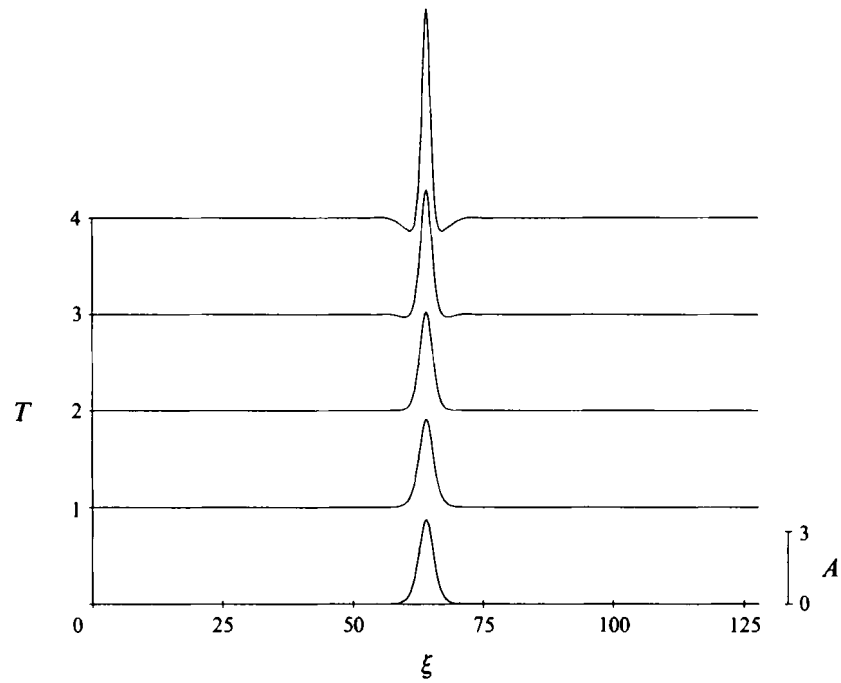

FIGURE 10. The explosive instability which occurs for initial lumps of solitary wave form whose amplitude exceeds 3.

fragments left by each anomaly will move relative to each other and collide. We describe in this section a set of numerical experiments dealing with the collision of solitary waves.

Before examining these experiments, it is useful to ask the following question. Suppose we start at $T = 0$ with a disturbance of the form

$$A = A_0 \operatorname{sech}^2 \lambda x, \quad \mathrm{d}A/\mathrm{d}T = 0, \quad T = 0, \tag{6.1}$$

but where $A_0 > 3$ so that no solitary wave solution is consistent with (4.5*a*, *b*). Figure 10 shows the result of such a trial with $A_0 = 3.5$, and it is entirely typical of situations where solitary wave shapes have a mass greater than the mass of a solitary wave of amplitude $A_0 = 3$. That is, if

$$m > m_S(A_0 = 3) = 12, \tag{6.2}$$

an explosive instability occurs.

The collisions we investigate are of two types: either slow, overtaking collisions or relatively fast head-on collisions. It is important to recall that the fundamental eigenvalue problem sets a definite speed for the frame in which (4.4) applies. Hence, there is a distinguishable difference between overtaking and colliding events that cannot be trivially eliminated by a Galilean transformation.

Our initial expectation was that the former, in which the time of interaction of the two pulses is longer, would be more dangerous to fragmentation. This turns out not to be the case.

Figure 11 shows a thoroughly typical example of a smaller ($A_0 = 1$), wider solitary wave overtaking a larger ($A_0 = 2$), narrower more slowly moving solitary wave. Initially well separated, they begin to merge at $T \sim 240$, briefly coalesce, and then with an exchange of identities or a tunnelling of one through the other, the faster, smaller,

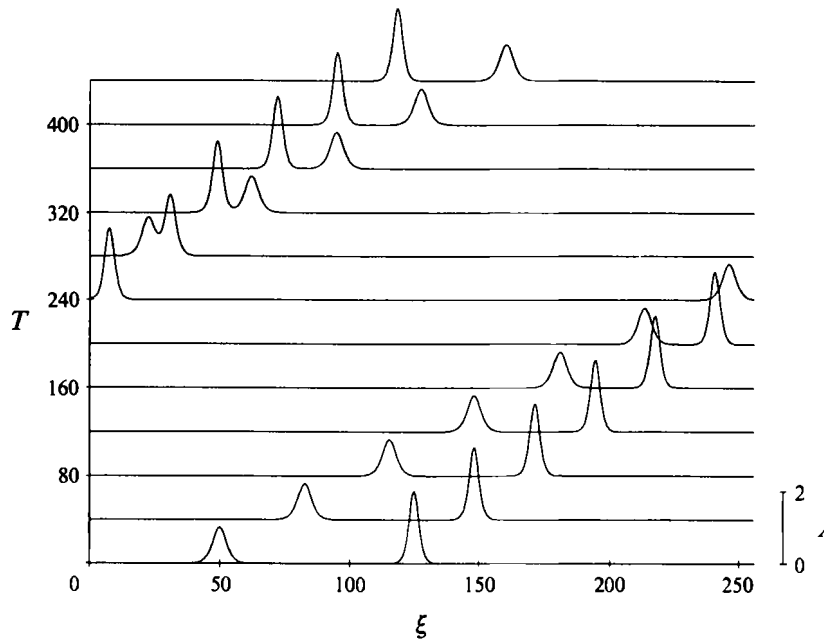

FIGURE 11. The stable overtaking interaction of two solitary waves; $A_1 = 1$, $A_2 = 2$.

solitary wave emerges at $T \sim 320$, and two disturbances with the same shape as the initial pair smoothly separate. The interaction is entirely stable, but does result in a phase shift of each wave.

The situation is quite different for head-on collisions. In figure 12(*a*), we show the symmetrical collision of two solitary waves, each of amplitude unity, in a head-on collision. After coalescing at $T \sim 25$, the resulting single, stationary hump begins an explosive growth similar to the instability of figure 10.

The mass in each solitary wave is

$$m = (48A_0)^{\frac{1}{2}}, \tag{6.3}$$

which is 6.93 for $A_0 = 1$. Since mass is conserved during the collision, the mass of the coalesced lump is 13.86 and, therefore, exceeds the mass of the limiting solitary wave of amplitude 3 which has $m = 12$. Even for collisions that are not symmetric, we have found that the criterion that total mass not exceed 12 for stability is fairly well obeyed. Figure 12(*b*) shows the asymmetric collision of two waves of amplitudes 1 and 2, respectively, and again, the explosive instability occurs.

On the other hand, head-on collisions of solitary waves whose summed masses are less than 12 seem to be stable, as the example of figure 12(*c*) shows in which $A_1 = A_2 = 0.5$, so that $m(A_1)+m(A_2) = 9.798 < 12$. The two solitary waves pass through each other with no change of shape in a stable interaction similar to the overtaking condition.

Consider now two waves of amplitude A_1 and A_2 which coalesce to form a lump which we approximate as, instantaneously, a single solitary wave of amplitude A_3. Then conservation of mass implies

$$A_1^{\frac{1}{2}} + A_2^{\frac{1}{2}} = A_3^{\frac{1}{2}}, \tag{6.4}$$

or

$$A_2 = A_3 + A_1 - 2(A_1 A_3)^{\frac{1}{2}}. \tag{6.5}$$

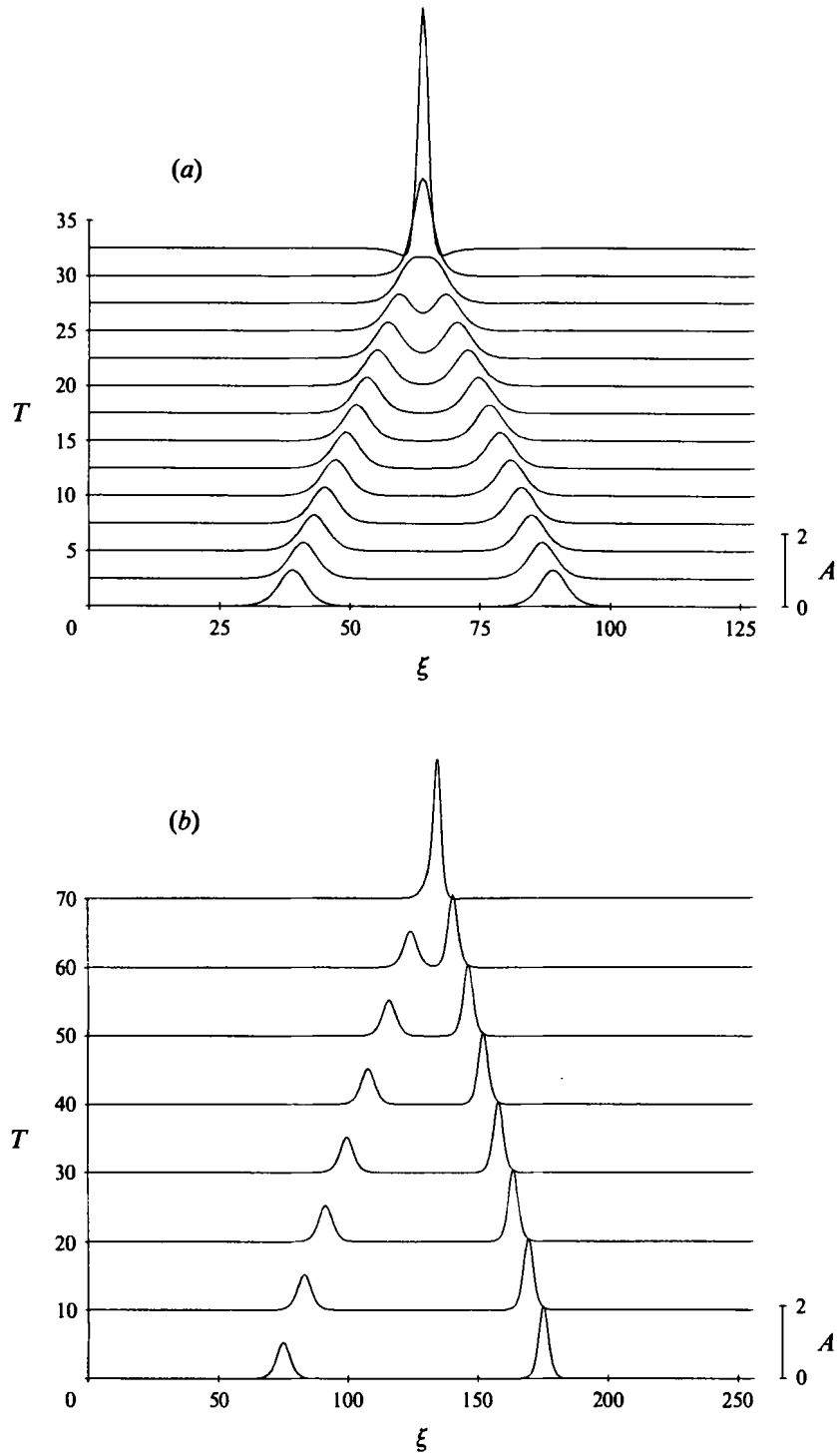

FIGURE 12(*a*,*b*). For caption see facing page.

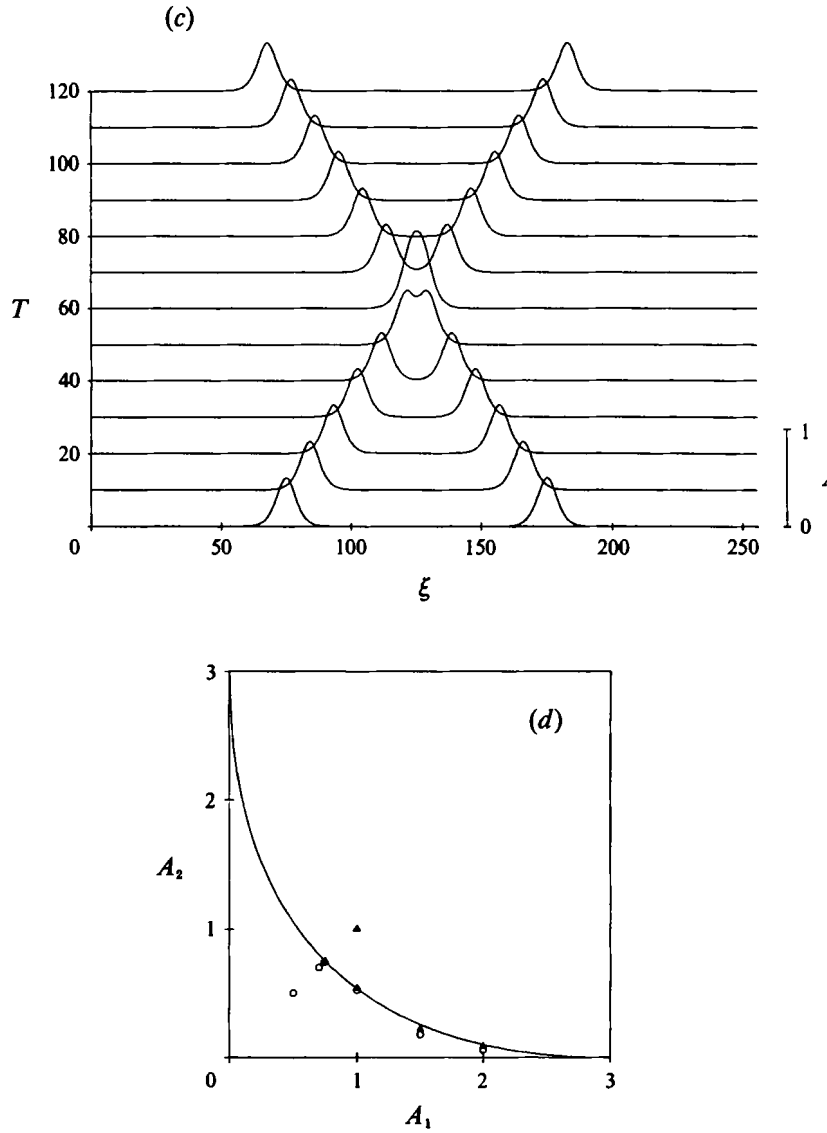

FIGURE 12. (*a*) The explosive instability of two equal solitary waves ($A_1 = A_2 = 1.0$), suffering a head-on collision. (*b*) As in (*a*) except the initial condition is not symmetric ($A_1 = 1, A_2 = 2$). (*c*) Stable head-on collision of smaller-amplitude waves ($A_1 = A_2 = 0.5$). (*d*) The stability diagram described in the text. The numerical results are indicated by circles for stable interaction and triangles for explosive instability.

If we provisionally assert that the critical lump size for instability is $A_3 = 3$ then the threshold of instability of two colliding solitary waves would be given by

$$A_2 = A_1 - 2(3A_1)^{\frac{1}{2}} + 3, \tag{6.6}$$

and this threshold curve is shown in figure 12(*d*) along with the results of numerical runs. We have found that (6.6) predicts fairly well the boundary between unstable and stable interactions between colliding solitary waves. There is some departure from the criterion (6.6) when one of the solitary waves has a very small initial amplitude, for then the resulting instability requires a long time to develop.

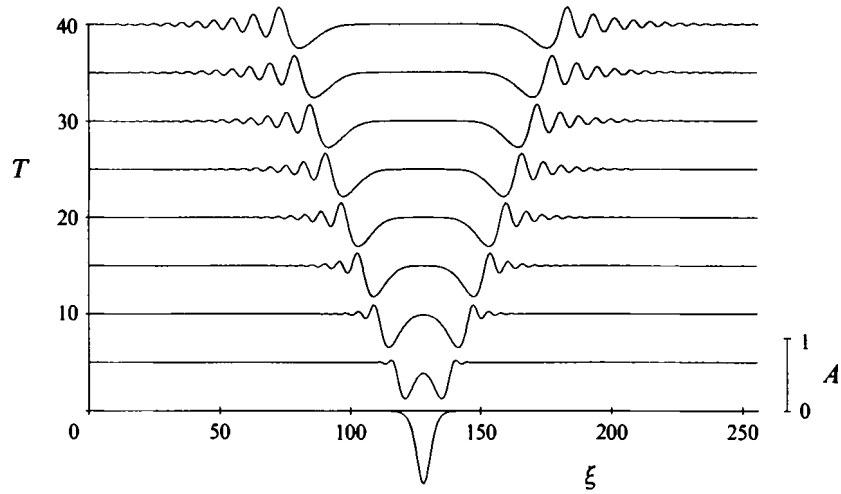

FIGURE 13. The spontaneous breakdown into two wave packets of an initial solitary wave of 'wrong' sign.

In general then, should fragments of previous solitary waves which have fissioned collide, the fragments, if large enough, could produce a locally large-amplitude instability. It will take further analysis beyond the scope of the present study to discover the final state achieved after the explosive instability carries the motion field beyond the region of validity of our asymptotic analysis.

7. General initial conditions

If the initial disturbance is not of solitary wave form, basically three resulting scenarios of behaviour have been found. In the first case, the initial disturbance can simply scatter and degenerate into a nonlinear wave packet. Figure 13 shows the evolution in time of an initial condition that is in every way consistent with the analytic nonlinear solitary wave except that its amplitude is negative ($m_4 A_0 < 0$) when it should be positive. The disturbance quickly breaks down and disperses as two wave packets.

If the amplitude is positive ($m_4 A_0 > 0$), but the shape is not that of solitary wave, our calculations have shown that the initial lump of the form, for example,

$$A = A_0 e^{-(\lambda\xi)^2}, \tag{7.1}$$

can either fission into two solitary waves as in figure 14(*a*) or, at the same value of λ but higher amplitude, succumb to the explosive instability as shown in figure 14(*b*). For the Gaussian initial distribution (7.1), we have found an empirical threshold between splitting and explosive instability in which (figure 15*a*) the critical transition to explosive behaviour, rather than splitting, is essentially linear in λ. That is, narrow initial pulses must have larger amplitude to achieve explosive amplitude growth. This is not, however, simply a question of total mass as in the case of solitary wave interactions. As figure 15(*b*) shows, the threshold mass for explosive instability depends on the shape parameter, i.e. the criterion distinguishing explosive from splitting instability is not based only on initial mass but is also shape-depednent.

In fact, if the initial data have essentially no mass, a rather interesting evolution can occur. Figure 16 shows the evolution of an initial condition consisting of a plane wave packet, i.e.

$$A = a_d \sin k_d \xi, \tag{7.2}$$

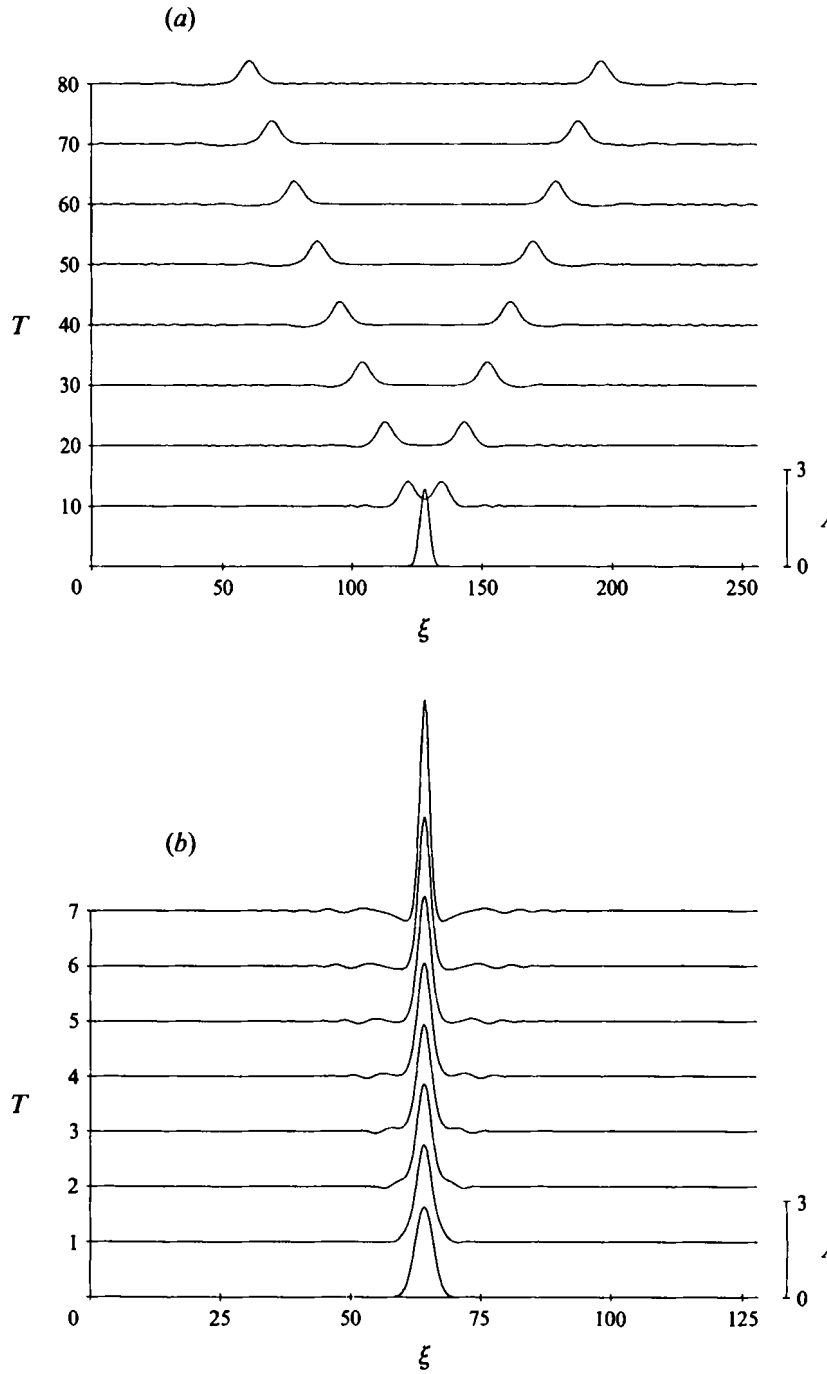

FIGURE 14. The evolution of an initially Gaussian lump to either (*a*) separating solitary waves, or (*b*) the narrowing of the lump and the catastrophic growth of the amplitude.

but 'windowed' such that A vanishes for large ξ. For example, in figure 16, the wavelength of the plane wave is 19, and it is windowed in a ξ-interval of $O(100)$. The initial packet splits and each piece propagates to large $|\xi|$. As described above, the linear plane waves always move faster than the solitary waves. What is evident in figure

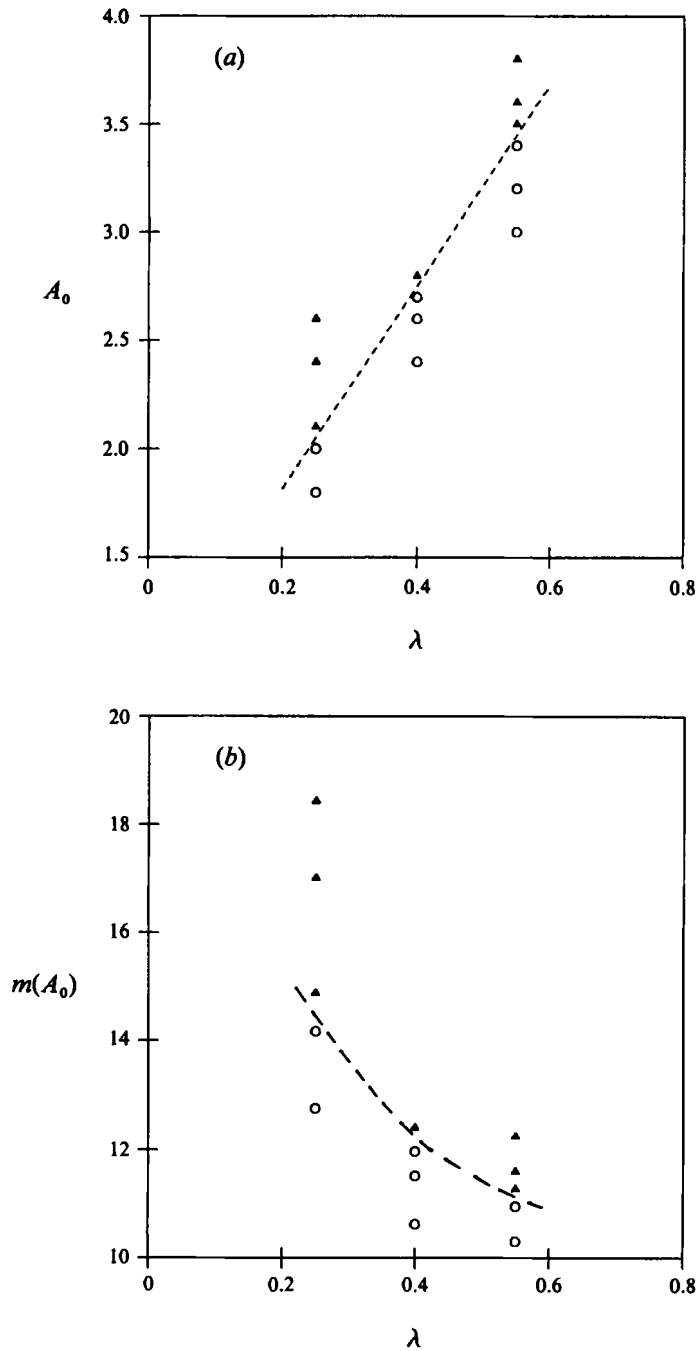

FIGURE 15. The threshold between explosive and fission behaviour of an original Gaussian lump $A(\xi, 0) = A_0 e^{-(\lambda\xi)^2}$. (*a*) A_0 *vs.* λ. Note the linear relation for the threshold. (*b*) $m(A_0)$ at the threshold *vs.* λ. Note that $m(A_0)$ is not sufficient to distinguish the two behaviours. In both figures the triangles correspond to runs which grew explosively and the circles to separating waves.

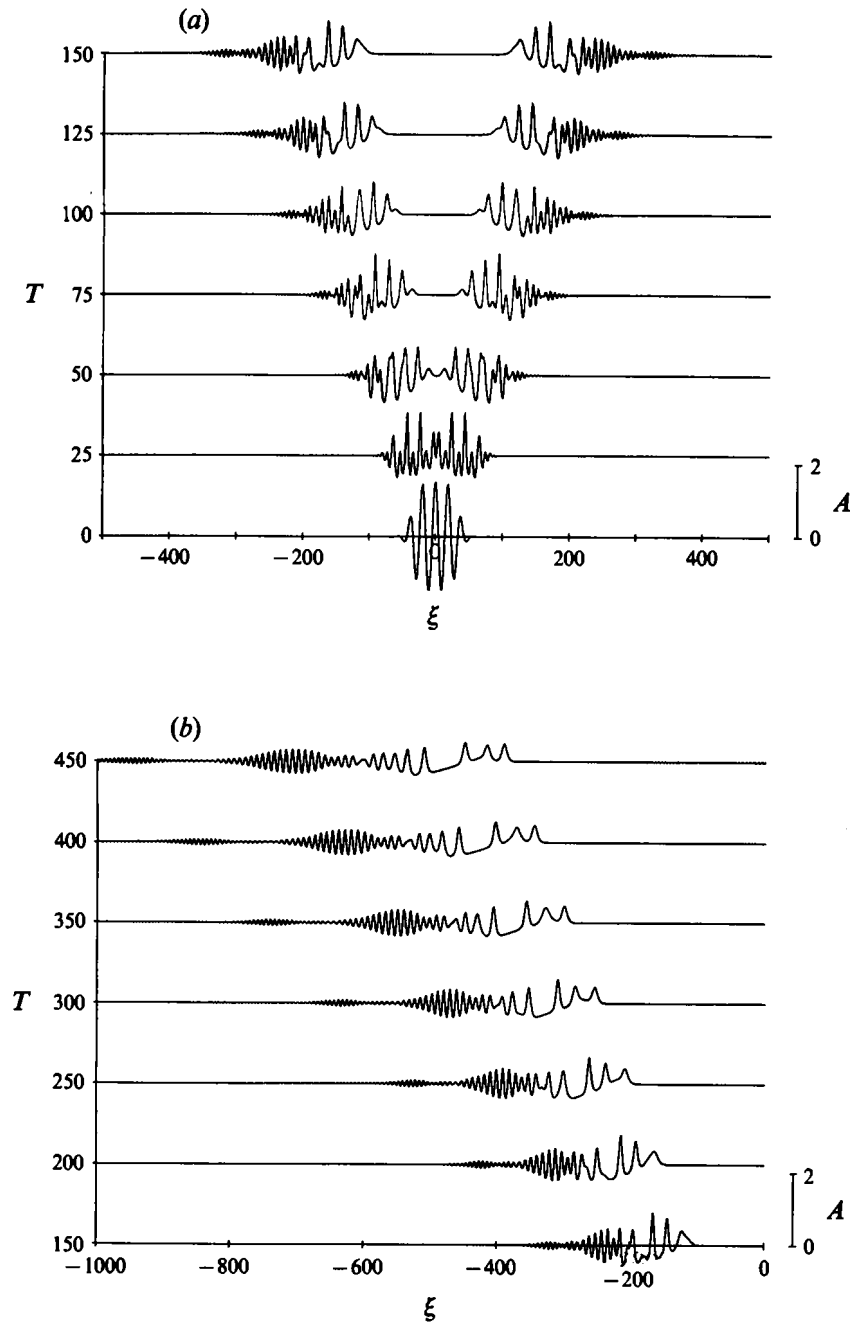

FIGURE 16. (*a*) The evolution in time of a nonlinear wave packet into two wave trains followed by an evolving sequence of solitary waves. (*b*) For $t > 150$, we show only the left-hand moving disturbance.

16 is the development in the lee of each plane wave pulse of a series of slower solitary waves being left behind by the dispersing plane wave disturbances. This is a particularly significant result because it indicates that it is not necessary to start with shapes close to an isolated disturbance to achieve an anomaly. A solitary wave can evolve as the end state of a more general initial disturbance distribution.

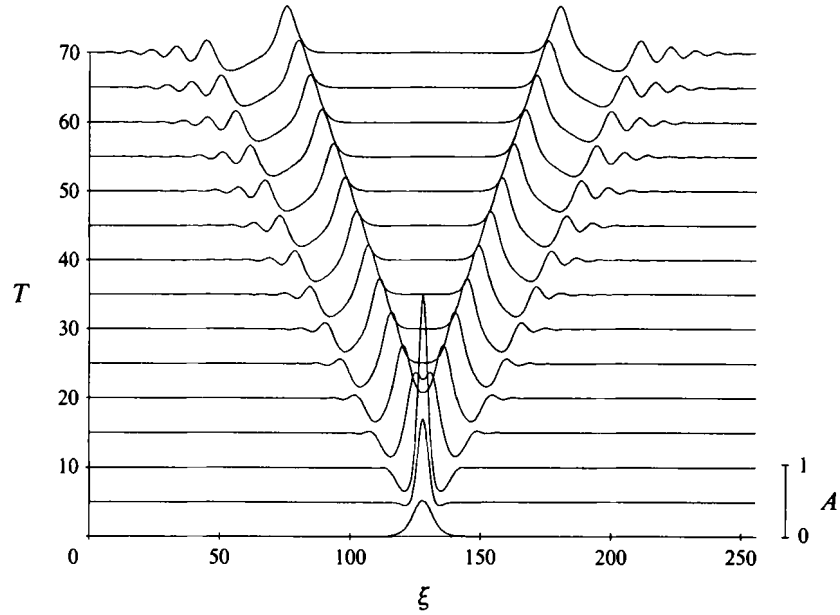

FIGURE 17. The disturbance history when the background flow changes from unstable to stable. After initial growth of the seed the lump splits into two solitary waves.

8. Transition events: development of solitary solutions

We have seen how already-formed finite-amplitude disturbances will further evolve under the influence of dispersion and nonlinearity in that part of parameter space (quadrant 4 of figure 1) in which the background flow is slightly subcritical. We describe here a possible scenario by which such finite-amplitude disturbances may be formed. To do so, we take advantage of the previously noted fact that m_3 can be considered a function of T. We imagine that initially our background state is slightly supercritical so that, for $m_1 > 0$, we have $m_3 > 0$. Then as time goes on, we allow the background flow to stabilize by specifying that $m_3(T)$ passes through zero and becomes negative. In particular, we suppose that

$$m_1 = m_2 = m_4 = 1, \tag{8.1}$$

while

$$m_3 = \begin{cases} 1-0.2T; & T < 10, \\ -1; & T > 10, \end{cases} \tag{8.2}$$

with an initial condition consisting of a small disturbance

$$A = A_0 \operatorname{sech}^2 \lambda x, \tag{8.3}$$

where $A_0 = 0.5$; $\lambda = 0.204$. Although we are specifying a temporal change in the background stability, it is perhaps more relevant (although more complex) to think of the disturbance as transiting from a region in ξ of background instability to one of stability. However, in strict accordance with the development of our amplitude equation, we must formally consider this to occur instead in time.

Figure 17 shows the development of an isolated initial perturbation when m_3 is given by (8.2). For as long as the background flow is unstable, the disturbance grows exponentially in place. Even though m_3 is a function of time, and the background flow is unstable, the disturbance mass is still conserved. This requires, as shown in the figure,

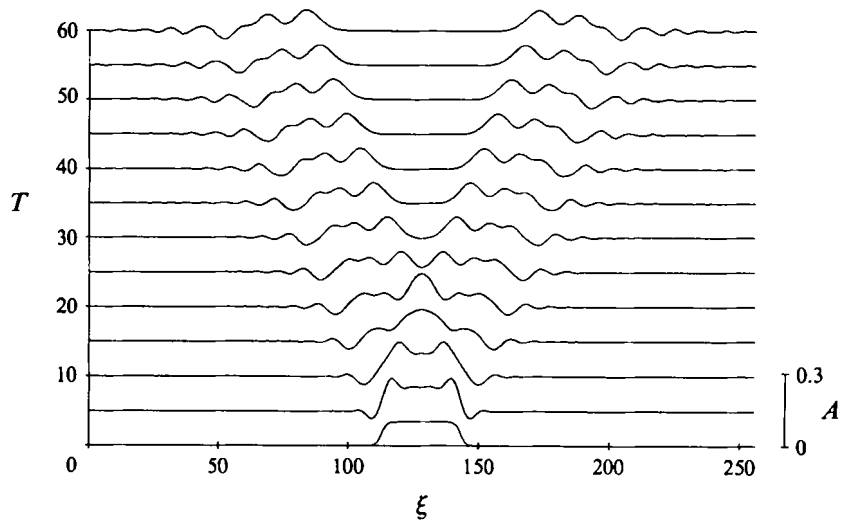

FIGURE 18. As in figure 17 except the initial disturbance is not of solitary wave shape.

the disturbance to narrow as it grows. After $T = 5$, the background flow becomes stable and the flow parameter m_3 makes the transition from the first to the fourth quadrant of figure 1. The value of m_3 is then held fixed for $T > 10$ at the subcritical value, $m_3 = -1$. The disturbance is seen to fission, forming two large lumps plus preceding nonlinear wave trains. Each lump, with amplitude $A_0 \sim 0.65$ moves with a speed $u = 0.88$, in excellent agreement with the solitary wave solution (4.5*a*). We thus suggest that small-disturbance seeds can grow to finite amplitude in an unstable regime, and if the evolved shape is appropriate, metamorphose into solitary waves should the background flow become stable or should the disturbance enter a zone of stable background flow. The initial seed need not be of solitary wave shape. Figure 18 shows the emergence, after fission, of four solitary waves, two in each direction, from an initial distribution consisting essentially of a plateau in ξ.

9. Discussion

We have taken the original steady-state theory of Malguzzi & Malanotte-Rizzoli (1985), and embedded it in a time-dependent theory for a marginally stable atmosphere (or ocean). In our development, the fundamental eigenvalue problem, (2.15), for the meridional structure has as its eigenvalue the $O(1)$ zonal translation speed, c_0, of the finite-amplitude anomaly. In general, the eigenvalue problem yields two values of c_0, and we have chosen to work in that part of the parameter space where a coalescence of the eigenvalues occurs as a manifestation of the marginal stability of the basic zonal flow in which the anomaly develops. Both nonlinear effects and departures of the zonal flow structure from the precise marginal state lead to a slow drift with velocity u with respect to the frame moving with c_0. Thus for the solitary wave, we have as a complete representation in x and t:

$$\phi_n = A_0 \operatorname{sech}^2 \alpha\kappa[x - t(c_0 + (\mu/\alpha)u)]\, H_n(y), \tag{9.1}$$

where κ is $O(1)$, but where μ and α are small and $\mu = O(\alpha^2)$. Since $\alpha \ll 1$, it follows that, for stationary anomalies, the first requirement is that the parameters of the basic flow problem are such that $c_0 = 0$. This, in principle, can always be obtained after coalescence by the imposition of a uniform barotropic flow on the system. This

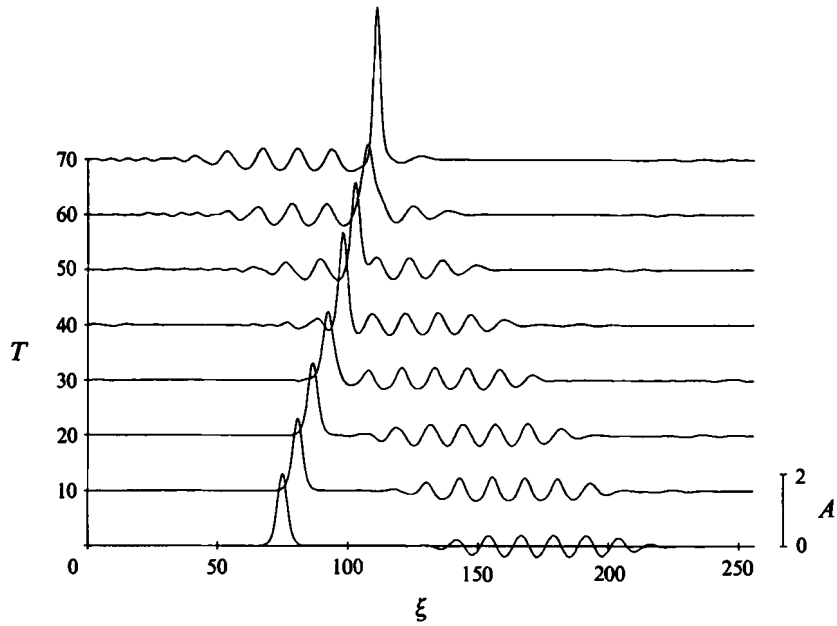

FIGURE 19. The collision of an otherwise stable solitary wave ($A_0 = 2$) with a nonlinear wave train. The amplitude of the crests in the wave train are large enough to induce the explosive instability of the solitary wave.

criterion is identical to that of Malguzzi & Malanotte-Rizzoli, and our development is consistent with theirs to that extent. However, to have a completely stationary solution, u must also be zero, else a slow drift of the anomaly will occur. For $u = 0$ a particular condition (3.2) must hold between the amplitude A_0 and the width κ of the solitary wave again in agreement with the original steady theory. We emphasize again that our development also contains Haines & Malanotte-Rizzoli's description of jet streaks in addition to split jet anomalies.

The solitary wave itself can only be found in that portion of parameter space in which the background zonal flow is *stable* (although in our case, only marginally so). However, the stationary solution, previously proposed as a permanent coherent structure, is unstable even with the conditions of background flow subcriticality. Our calculations show that the solitary wave either fissions and emits slowly moving solitary waves both eastward and westward or contracts and implodes developing a narrowness and amplitude finally inconsistent with our asymptotic theory. Which of the two occurs depends sensitively on the sign of the ambient background disturbances. Hence the mode of self-destruction of the anomaly sensitively depends on initial data. We think, first of all, that the natural slow decay of the stationary anomaly is an attractive feature of the theory giving a long but finite lifetime to nonlinear anomalies in atmospheric currents. Our asymptotic theory is adequate to describe the fission process. The implosion and strong peaking scenario confronts us with a process that we are unable to legitimately follow beyond a certain point. We plan in the future to return to the full quasi-geostrophic potential vorticity equation to see how the explosive amplitude growth and the catastrophic thinning of the anomaly are halted.

The solitary waves below a certain critical amplitude (see figure 6) are stable to small disturbances. They are robust, however, only when undergoing certain restricted interactions. In particular, head-on collisions of solitary waves will again lead to further instabilities if the instantaneous summed mass of the disturbances, e.g. the area

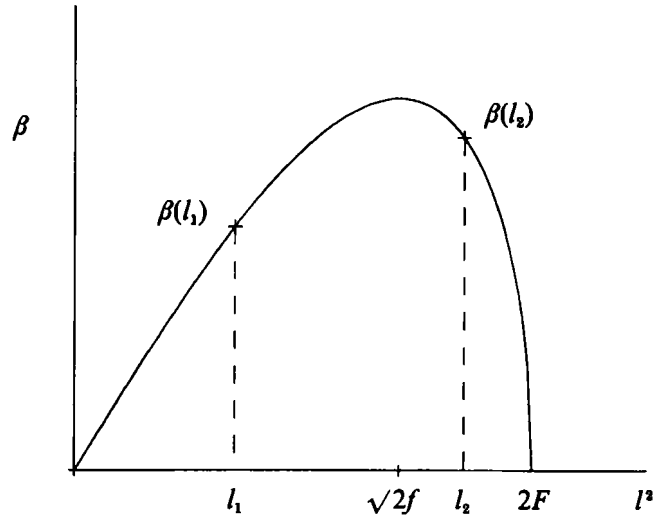

FIGURE 20. A curve showing the non-dimensional critical β *vs.* l for the Phillips two-layer model as $k^2 \to 0$. The figure shows a case in which the second cross-stream eigenmode will be more dangerous than the first.

under the $A(x)$ curve, exceeds a critical value. Thus the coherent structures are easily disposed of if they are disturbed in such a way that the peak amplitude of the solitary wave plus that of the disturbance even momentarily resembles a solitary lump whose amplitude exceeds a critical value. Figure 19, for example, shows an otherwise stable solitary wave being struck head-on by a nonlinear wave packet. Although the wave packet has essentially no net mass, the sum of the solitary wave and one of the wave crests in the packet is enough to send the solitary wave into irreversible explosive growth.

As in the previous steady-state theories, it would appear fortuitous that the second meridional eigenfunction should be more important than the first. We focus attention on the second cross-stream mode because its dipolar structure is suggested by the observed dipolar blocking patterns in the atmosphere. It might well be asked how we can focus on the second cross-stream mode and require it to be marginally critical and ignore the gravest mode. Surely, were the gravest mode frankly unstable, this would argue against the relevance of the second mode. Figure 20 shows a schematic of the marginal curve for the two-layer model yielding the critical β for stability as a function of cross-stream wave number for the case where the horizontal shear is negligible. Since l is quantized, only a few l values are possible within the unstable range $l^2 < 2F$. In the example shown, the gravest mode has $l = l_1$ on the long-wave side ($l^2 < \sqrt{2F}$) with $\beta(l_1) < \beta(l_2)$ where l_2 is the second cross-stream wavenumber here shown on the short-wave side (i.e. in the right-hand part of figure 1). Hence in this case the second mode would, in fact, be the more 'dangerous'.

The time-dependent theory has established a larger dynamical setting in which to consider coherent anomalies in atmospheric flow patterns. It emphasizes the richer dynamics the anomalies can experience and underscores the transient and surprisingly fragile character of the previously examined steady solutions when the background flow, while near its ordinary criticality condition for instability, is definitely stable. It will be of considerable interest to numerically and analytically extend these results by removing the asymptotic requirements of the present analysis. Such work is in progress.

This work was supported in part by a grant from the National Science Foundation's Division of Atmospheric Sciences (J.P.) and a grant from NSF's Division of Ocean Sciences (K.R.H.). The numerical computations were done on the NCAR CRAY Y-MP.

Appendix

If the parameters of the background flow are such that the coalescence of roots (2.18) does not take place, this implies that the background flow is distant from the marginal curve. If the flow is strongly supercritical, we cannot expect disturbances of fixed shape to dominate the solution. Thus in the non-coalescing regime, we are describing firmly subcritical, stable flows. When coalescence does not occur, (2.22) will not be satisfied for non-trivial disturbances. In such a case, rather than (2.20) we must choose the equality

$$\mu = O(\alpha\Delta, \alpha^3, \epsilon\alpha). \tag{A 1}$$

Proceeding as in §2, the solvability condition then yields for A the governing equation

$$n_1 \frac{\partial A}{\partial T} - \frac{\alpha^3}{\mu} m_2 \frac{\partial^3 A}{\partial \xi^3} - \frac{\alpha\Delta m_3}{\mu} \frac{\partial A}{\partial \xi} - \frac{\epsilon\alpha}{2\mu} m_4 \frac{\partial}{\partial \xi} A^2 = 0, \tag{A 2}$$

where m_2, m_3 and m_4 are given as in (2.28) and

$$n_1 = \sum_{n=1}^{2} \int_0^1 \mathrm{d}y \frac{H_n^2}{(U_n^{(0)} - c_0)^2} \frac{\partial Q_n^{(0)}}{\partial y}.$$

Solitary wave solutions of (A 2) of form

$$A = A_0 \operatorname{sech}^2 \kappa(\xi - uT)$$

are possible if

$$\kappa^2 = \frac{m_4}{m_2} \frac{A_0}{12} \tag{A 3}$$

as in (3.2*b*), while the solitary wave moves in only a single direction with respect to a frame moving with speed c_0 (which may be either $c_0^{(1)}$ or $c_0^{(2)}$) at the rate

$$u = -\frac{m_3}{n_1} - \frac{1}{3} \frac{m_4}{n_1} A_0. \tag{A 4}$$

If $m_3 < 0$ as in the stable examples of §3, and if the potential vorticity gradient is positive in each layer (rendering the background flow stable), then n_1 will be positive, as will be $-m_3/n_1$. Then completely stationary solutions are possible when

$$m_4 A_0 = 3m_3, \tag{A 5}$$

which is the criterion of Malguzzi & Malanotte-Rizzoli. Given the classical KdV nature of (A 2), we conclude that in this case of firmly subcritical background flow, the stationary solitary wave will be stable.

REFERENCES

DEININGER, E. 1980 Baroclinically growing solitary waves. In *Notes of Geophysical Fluid Dynamics Summer Study Program* (G. Veronis, Director), pp. 142–154. Woods Hole Oceanographic Institution, Woods Hole, MA.

FORNBERG, B. & WHITHAM, G. B. 1978 A numerical and theoretical study of certain nonlinear wave phenomena. *Phil. Trans. R. Soc. Lond.* A **289**, 373–404.

HAINES, K. & MALANOTTE-RIZZOLI, P. 1991 Isolated anomalies in westerly jet streams: A unified approach. *J. Atmos. Sci.* **48**, 510–526.

HAINES, K. & MARSHALL, J. C. 1987 Eddy-forced coherent structures as a prototype of atmospheric blocking. *Q. J. R. Met. Soc.* **113**, 681–704.

MALGUZZI, P. & MALANOTTE-RIZZOLI, P. 1985 Coherent structures in a baroclinic atmosphere. Part II: A truncated model approach. *J. Atmos. Sci.* **42**, 2463–2472.

PHILLIPS, N. A. 1954 Energy transformations and meridional circulations associated with simple baroclinic waves in a two-level, quasi-geostrophic model. *Tellus* **6**, 273–286.